

1     **Development functional characterization of alginate dressing as potential**  
2                     **protein delivery system for wound healing**

3     Frederick U. Momoh<sup>a,1</sup>, Joshua S. Boateng<sup>a#,1</sup>, Simon C.W. Richardson<sup>b</sup>, Babur Z.  
4     Chowdhry<sup>b</sup>, John C. Mitchell<sup>a</sup>

5

6     <sup>a</sup> Department of Pharmaceutical Chemical and Environmental Sciences, Faculty of  
7     Engineering and Science, University of Greenwich at Medway, Central Avenue, Chatham  
8     Maritime, ME4 4TB, Kent, UK.

9     <sup>b</sup> Department of Life and Sports Sciences, Faculty of Engineering and Science, University of  
10    Greenwich at Medway, Central Avenue, Chatham Maritime, ME4 4TB, Kent, UK.

11

12    # Correspondence: Dr Joshua Boateng ([J.S.Boateng@gre.ac.uk](mailto:J.S.Boateng@gre.ac.uk); [joshboat40@gmail.com](mailto:joshboat40@gmail.com))

13

14    <sup>1</sup>Joint First Authors

15

16

17

18

19

20

21

22

23

24

## ABSTRACT

This study aimed to develop and characterize stable films as potential protein delivery dressings to wounds. Films were prepared from aqueous gels of sodium alginate (SA) and glycerol (GLY) (SA:GLY 1:0, 1:1, 1:2, 2:3, 2:1, 4:3) , . Purified recombinant glutathione-s-transferase (GST), green fluorescent protein (GFP) and GST fused in frame to GFP (GST-GFP) (model proteins) were characterized (SDS PAGE, Western blotting, immune-detection, and high sensitivity differential scanning calorimetry) and loaded (3.3, 6.6 and 30.2 mg/g of film) into SA:GLY 1:2 film. These were characterized using texture analysis, differential scanning calorimetry (DSC), thermogravimetric analysis (TGA), scanning electron microscopy, swelling, adhesion, dissolution and circular dichroism (CD). The protein loaded dressings were uniform, with a good balance between flexibility and toughness. The films showed ideal moisture content required for protein conformation (TGA), interactions between proteins and film components (DSC), indicating stability which was confirmed by CD. Swelling and adhesion showed that formulations containing 6.6mg/g of protein possessed ideal characteristics and used for in vitro dissolution studies. Protein release was rapid initially and sustained over 72 hours and data fitted to various kinetic equations showed release followed zero-order and Fickian diffusion. The results demonstrate the potential of SA dressings for delivering therapeutic proteins to wounds

**Key words:** Alginate dressing, GST-GFP Proteins, Wound healing.

## 53        **1. Introduction**

54        A wound is defined as a disruption of normal anatomic structure and physiology [1] of a tissue  
55        and represents damage of natural defense barriers which encourages invasion by  
56        microorganisms [2]. The process of wound regeneration is a complex combination of matrix  
57        destruction and reorganization [3] which requires well-orchestrated processes that lead to the  
58        repair of injured tissues [4]. These processes are integrations of complex biological and  
59        molecular events culminating in cell migration, proliferation, extracellular matrix deposition  
60        and the remodeling of scar tissues [5]. This process is driven by numerous cellular mediators  
61        including cytokines, nitric oxide, and various growth factors [6] (most of them proteins) which  
62        stimulate cell division, migration, differentiation, protein expression and enzyme production.  
63        Their wound healing properties are mediated through the stimulation of angiogenesis and  
64        cellular proliferation [7] which affects the production and degradation of the extracellular  
65        matrix and also plays a role in cell inflammation and fibroblast activity [8]. The field of biologic  
66        wound products aims to accelerate healing by augmenting or modulating these inflammatory  
67        mediators. These products have experienced remarkable growth as our understanding of the  
68        wound healing response has increased [6], coupled with the large number of recombinant  
69        proteins being investigated for therapeutic applications.

70

71        Alginate dressings are bioactive formulations composed of a polysaccharide polymer called  
72        alginic acid which contains guluronic and mannuronic acid units [9]. These dressings can occur  
73        in the form of fibers rich in mannuronic acid (e.g. Sorbsan<sup>TM</sup>) which form flexible gels upon  
74        hydration or those rich in guluronic acid residues which form firmer gels upon exudate  
75        absorption (e.g. Kaltostat<sup>TM</sup>). Alginate dressings are non-toxic and aid in hemostasis as part of  
76        the wound healing process [10-13]. In addition, they activate human macrophages to produce  
77        tumor necrosis factor- $\alpha$  (TNF $\alpha$ ) which initiates inflammatory signals [14].

78           The therapeutic effects of large macromolecules such as proteins and growth factors  
79 are limited by their low bioavailability and poor stability, whilst multiple injections can result  
80 in poor patient compliance. Therefore, drug delivery systems such as adhesive film dressings  
81 present a valid approach to overcome these limitations since films are simple, easy to prepare  
82 and characterize. Further, being in the dry state, it's easy to incorporate and stabilize labile  
83 proteins without the need for more expensive drying approaches such as freeze-drying,  
84 however, this depends on the type of protein and the temperature of drying. It has been  
85 proposed that films have potential to be used to deliver genetic and protein based molecules to  
86 wound sites [15]. Alginate film dressings are easily biodegradable and painlessly removed via  
87 saline irrigation when trapped in the wound thus preventing damage to newly formed  
88 granulation tissue [16, 17].

89

90           The requirement of wound management products with ideal characteristics has necessitated the  
91 need for advanced formulations such as alginate having improved physico-mechanical  
92 properties and general functional performance such as bioadhesion, but which are also able to  
93 actively take part in the wound healing process [2, 18]. In this study, we report on the use of  
94 film dressings formulated from two readily biodegradable materials; SA (film forming  
95 polymer) and GLY (plasticizer), loaded with recombinant proteins (GST, GFP and GST-GFP)  
96 as model protein drugs for potential wound healing. Films were prepared from aqueous gels of  
97 SA by solvent casting and characterized for functional characteristics expected for wound  
98 dressings.

99

## 100           **2. Experimental**

### 101           2.1 Materials

102 Nitrocellulose membrane, thiazolyl blue tetrazolium bromide, polyethyleneimine (branched,  
103 Mn 60000), dextran (Mw 35000-45000), isopropyl $\beta$ -D-1-thiogalactopyranoside (IPTG), L-  
104 glutathione, guanidine hydrochloride, MTT reagent [3-(4,5-dimethylthiazol-2-yl)-2,5-  
105 diphenyltetrazolium bromide] were obtained from Sigma (Gillingham, UK). Tryptone was  
106 obtained from Oxoid, (Hampshire, UK). Yeast extract, dimethyl sulfoxide (DMSO),  
107 trimethylamine and sodium chloride were obtained from Fisher Scientific, (Leicestershire,  
108 UK). Glutathione sepharose 4B, ECL Western blotting detector reagents 1 and 2 were obtained  
109 from GE HealthCare, (Buckinghamshire, UK). Acrylamide/Bis 37.5:1 and Bradford reagent  
110 (1x) were obtained from Bio-Rad, (Hempstead, UK). Anti-rabbit immunoglobulin (IgG)-  
111 Horseradish peroxidase (HRP) conjugated and GFP were obtained from Invitrogen, (Paisley,  
112 UK). Anti-Rabbit IgG-HRP and GST were obtained from Abcam, (Cambridge, UK).  
113 Recombinant GST-GFP, GST and GFP were prepared in house (Richardson lab, University of  
114 Greenwich, UK). Sodium alginate [medium viscosity ( $\geq 2000$  cps) grade; M/G ratio of 1.56],  
115 glycerol and bovine serum albumin were all obtained from Sigma-Aldrich, (Gillingham, UK).  
116 Dulbecco's-modified eagle's medium (D-MEM), PBS, penicillin, streptomycin and glutamine  
117 were all obtained from Gibco, (Paisley, UK). Gelatin was obtained from Fluka Analytical,  
118 (Steinheim, Germany) and calcium chloride from Sigma Aldrich, (Steinheim, Germany).

119

## 120 2.2 Recombinant protein preparation, purification and characterization

121 The protein production, purification, immuno-detection and characterization were performed  
122 according to that previously reported [19, 20]. The eluted proteins (GST-GFP, GST and GFP)  
123 were sealed in cellulose acetate dialysis membrane and dialyzed against 4L of cold 1x PBS  
124 (4°C) overnight and changing the dialysis buffer every 2 hours afterwards with a minimum of  
125 4 changes of (1x) PBS. 15 $\mu$ L each of purified proteins [GST-GFP (5 $\mu$ g), GST (2mg) and GFP  
126 (1mg)] and controls [Spectra Multicolor broad range protein molecular weight ladder

127 (Fermentas, Cambridgeshire, UK) and bovine serum albumin (BSA) standards (75 $\mu$ g)] were  
128 loaded onto sodium dodecyl sulfate polyacrylamide gel electrophoresis (SDS PAGE) apparatus  
129 using 6M guanidine containing Laemmli buffer and 10% (v/v) beta-mercaptoethanol (BME),  
130 with a running buffer (1x) as per manufacturer's instructions. The loaded samples were  
131 resolved by applying 100V of direct current for 80 minutes. The gel was then stained with  
132 Coomassie brilliant blue for 2 hours and de-stained with Coomassie de-staining solution for  
133 another 2 hours, further soaked in 5% (v/v) glycerol / PBS and dried overnight using a gel  
134 drying kit (Promega, Hampshire, UK). Western blotting and immuno-detection was used to  
135 detect GFP-GST after separation and its immobilization on a solid phase-support. The  
136 experiment was performed in accordance with the manufacturer's instructions and as  
137 previously reported [19]. The specific protein bands were identified by superimposing the  
138 developed X-ray film onto the membrane in the cassette.

139

### 140 2.3 Preparation of film dressings

141 Various sodium alginate (SA) gels (1% w/w) with and without plasticizer (GLY) were  
142 employed to determine the best SA:GLY ratio (SA:GLY – 1:0, 1:1, 1:2, 2:3, 2:1, 4:3) for the  
143 preparation of uniform and homogeneous films. Drug loading was achieved by formulating the  
144 selected optimized film prepared above, with increasing drug concentrations (3.3, 6.6 and  
145 30.2mg/g of film) for all three proteins. SA was added gently and in small quantities (so as to  
146 avoid formation of lumps) to warm PBS (45°C) in a beaker and magnetically stirred until SA  
147 was completely dissolved (2 hours) to yield a clear homogeneous gel. The required amount of  
148 GLY was added to the gels with continuous stirring and heating for a further 1 hour. The model  
149 proteins were added to the optimized gel with gentle stirring and heating (45°C) until a  
150 homogenous mix was obtained (1 hour) and allowed to stand for 5 minutes (to remove air

151 bubbles). 30g was poured into Petri dishes (90mm diameter) and placed in a vacuum oven at  
152 40°C for 18 hours.

153

#### 154 2.4 MTT cytotoxicity assay

155 MTT assay was used to evaluate the cytotoxicity of the proteins and SA using dextran (Mw  
156 35,000-45,000) and polyethyleneimine PEI (branched, Mn ~ 60,000), as negative and positive  
157 controls respectively. Adherent Vero cells ( $1 \times 10^4$  cells/well) were used to seed a sterile, flat-  
158 bottom 96-well tissue culture plate containing Dulbecco's modified eagles medium (D-MEM)  
159 plus 10% (v/v) PBS, penicillin (100U/mL), streptomycin (100 $\mu$ g/mL) and glutamine  
160 (292 $\mu$ g/mL) (all under sterile conditions in a laminar hood) and incubated at 37°C in 5% (v/v)  
161 CO<sub>2</sub> for 24 hours. After 24 hours, the cells were exposed to either PEI, dextran, GST-GFP,  
162 GST and GFP (0-3mg/mL) in cell culture medium and incubated for 68 hours. 10 $\mu$ L (50 $\mu$ g) of  
163 MTT from stock solution (5mg/mL) was added to each well and the plate incubated for a further  
164 4 hours bringing the total incubation time to 72 hours. The contents of the plate were decanted  
165 and 100 $\mu$ L of DMSO was added to each well, incubated at room temperature for 30 minutes  
166 and the absorbance read on a Multi-scan EX Micro-plate photometer (Thermo Scientific,  
167 Essex, UK) at optical density (OD) 540nm. For SA however, adherent cells (Vero,  $1 \times 10^4$ )  
168 were exposed to SA gel after 24 hours. Data obtained was expressed as percentage cell viability  
169 (mean  $\pm$  standard deviation of the mean).

170

#### 171 2.5 Thermal analysis

##### 172 2.5.1 High sensitivity differential scanning calorimetry (HSDSC)

173 Preliminary characterization of the three model proteins were investigated using HSDSC  
174 determining the effect of pH (6.0, 7.5, 8.0 and 10.0), scan rate (0.5, 1.0 and 2.0°C/minute),  
175 protein concentrations (1.0, 2.5 and 5.0mg/mL) and reversibility. Degassed buffer and protein

176 solutions (800 $\mu$ L) were loaded into the reference and sample capillary cells using a calibrated  
177 automatic pipette. The cells were covered using rubber caps on same sides. The entire cell  
178 chamber was then tightly covered with the chamber lid to maintain constant pressure and  
179 samples analyzed with a pressure of 3 atmospheres, equilibration for 600 seconds and heating  
180 from 10°C to 95°C at the scan rates above. Prior to sample analyses (both water and buffer  
181 scans were run using the same parameters described above for analyzing the samples and  
182 showed a flat baseline which was used as reference scans before analyzing the samples.

183

#### 184 2.5.2 Differential scanning calorimetry (DSC)

185 Before analyzing of the samples, the DSC instrument was calibrated. Two different  
186 calibration experiments of the DSC machine (Q2000 TA instrument. The first experiment  
187 was performed in two stages i.e. determination of the cell resistance and capacitance. The  
188 determination of the cell resistance was performed with an empty cell. During this  
189 experiment, the cell was equilibrated at -90°C and held at this temperature (isothermal) for 5  
190 minutes, followed by a heating ramp from -90 to 400°C at a rate of 20°C/min. The  
191 determination of the cell capacitance, involved a similar experimental procedure as the cell  
192 resistance but sapphire discs of known weight and heat capacity were placed on the reference  
193 and sample cells. The second calibration experiment involved the determination of the cell  
194 constant and temperature calibration, which were obtained from a single experiment. In this  
195 experiment 1-5 mg of indium standard was pre-heated to which is above its melting transition  
196 temperature and held isothermally (5 minutes). The sample was then cooled to 100°C, held  
197 isothermally for a further 5 minutes and subjected to a heating ramp (10°C/min) to a  
198 temperature above the melting transition. The enthalpy of fusion was determined by  
199 integration and compared with the known value (28.71 J/g). The cell constant was calculated  
200 as the ratio between the experimentally determined and expected value and expected to be

201 between 1 and 1.2. The melting temperature was determined using the extrapolated onset  
202 value, and this was also compared with the known value (56.6°C) and the difference  
203 calculated for temperature accuracy.

204

205 DSC analysis was carried out on the starting materials (SA, GLY, GST, GFP and recombinant  
206 GST-GFP), formulated gels, as well as blank (non-protein) and protein loaded films. About  
207 19.0-20.0mg of GLY and gels, 3.3-8.0mg of SA, blank and protein loaded films were loaded  
208 into tarred Tzero aluminium pans which were crimped and hermetically sealed with one pin  
209 hole on the lid using a Tzero sample press (TA instruments, Crawley, UK). The analysis was  
210 performed using a Q2000 calorimeter (TA Instruments, UK), under inert nitrogen (N<sub>2</sub>) gas at  
211 a flow rate 50mL/minute, equilibration at -90°C, isothermal for 5 minutes and finally dynamic  
212 heating to 400°C at a heating rate of 10°C/minute.

213

### 214 2.5.3 Thermogravimetric analysis (TGA)

215 Tests were carried out on the starting materials [(SA, GLY), recombinant GST-GFP, GST and  
216 GFP (proteins) and the blank and protein loaded films. Analysis was carried out using a Q5000-  
217 IR TGA instrument (TA Instruments, Crawley, UK) by loading about 8.0 - 10.0mg (SA, GLY),  
218 9.5-10.0mg (proteins) and 3.0-3.6mg (film). The analysis was performed under inert nitrogen  
219 (N<sub>2</sub>) gas at a flow rate of 50mL/minute and dynamic heating from ambient (~25°C) to 600°C  
220 at a heating rate of 10°C/minute.

221

### 222 2.6 Tensile characterization

223 The tensile properties of the films (thickness, 0.1mm) were evaluated using a TA HD Plus  
224 (Stable Micro Systems Ltd, Surrey, UK) texture analyzer equipped with a 5kg load cell and a  
225 Texture Exponent-32<sup>®</sup> software program. The films (n=3), free of any physical defects (cracks

226 or tears) were cut into dumb-bell shapes and stretched between two tensile grips at a speed of  
227 6mm/s using a trigger force of 0.1N until films broke. The distance between the grips was 3mm  
228 whilst the width of the films was 1mm. Testing was first carried out on the blank (non-protein  
229 loaded) films with different plasticizer concentrations (SA:GLY, 1:0, 1:1, 1:2, 2:3, 2:1, 4:3) to  
230 determine the film with optimum mechanical (tensile) properties [15] for protein loading.  
231 Further to this, tests were carried out on protein loaded films. The tensile strength (brittleness),  
232 Young's modulus (rigidity/stiffness) and elongation (elasticity and flexibility) at break were  
233 determined from the force-time profiles using equations 1, 2 and 3.

234

$$235 \quad \text{Tensile strength } \left( \frac{\text{N}}{\text{mm}^2} \right) = \frac{\text{(Force at break (N))}}{\text{Initial cross sectional area (mm}^2\text{)}} \quad \text{Equation 1}$$

236

$$237 \quad \text{Elastic Modulus (mPa)} = \frac{\text{Slope}}{\text{Initial cross sectional area (mm}^2\text{)} \times \text{cross-head speed } \left( \frac{\text{mm}}{\text{s}} \right)} \quad \text{Equation 2}$$

238

$$239 \quad \text{Elongation at break (\%)} = \frac{\text{increase in length (mm) at break}}{\text{initial film length (mm)}} \times 100 \quad \text{Equation 3}$$

240

## 241 2.7 Scanning electron microscopy (SEM)

242 This was used to evaluate the surface morphology and topography of the films with and without  
243 proteins. Films were cut into rectangular (3x5mm) pieces and placed on the exposed side of a  
244 double-sided carbon adhesive tape stuck onto aluminum stubs (Agar Scientific, Essex, UK).  
245 Images were acquired using a Hitachi SU 8030 FEG-SEM (Hitachi High-Technologies, Tokyo,  
246 Japan) by generating secondary electrons at an accelerating voltage of 2kV and working  
247 distance of 15mm and magnification of x50.

248

## 249 2.8 Hydration and swelling

250 The swelling capacity of the formulated blank and protein loaded films were determined in  
251 simulated wound fluid (SWF) containing 0.02M calcium chloride, 0.4M sodium chloride,  
252 0.08M tris-methylamine and 2% (w/v) bovine serum albumin in deionized water [2]. The pH  
253 was adjusted to 7.5 using 2M HCl, mimicking chronic wound with pH reported to be in the  
254 range of 7.2 to 8.9 [21]. Films were cut into 2x2 cm strips, weighed and immersed in SWF  
255 (10mL). The weight change of the hydrated films was determined every 15 minutes for 120  
256 minutes. Hydrated films (n = 3) were blotted carefully with filter paper to removes excess SWF  
257 on the surface and reweighed immediately on an electronic balance. The percentage swelling  
258 index (%Is) was calculated from equation 4.

$$259 \quad \%Is = (Ws - Wd) / Wd \times 100 \quad \text{(Equation 4)}$$

260 Where Ws is the weight of films after hydration and Wd is the weight of films before hydration.

261

## 262 2.9 In vitro wound adhesion

263 In vitro wound adhesion test was carried out on the blank and protein loaded films using a  
264 TA HD plus Texture Analyzer (Stable Micro System, Surrey, UK) fitted with a 5kg load cell  
265 in tension mode. Films (n=4) were cut to square strips (2x2cm) and attached to a 75mm  
266 diameter probe using a double sided adhesive tape. Prior to testing, 20g of 6.67% (w/v) gelatin  
267 was poured into a Petri dish (90mm in diameter) and allowed to set at 4°C overnight. 500µL of  
268 SWF (pH 7.5) was spread evenly using an agar plate spreader so as to simulate a wound  
269 surface<sup>2</sup>. The films were kept in contact with the gelatin solution for 1 minute before  
270 detachment. The probe was set at a pre-test speed of 0.5mm/s, test speed of 0.5mm/s, a post-  
271 test speed of 1mm/s, and an applied force of 1N. The peak adhesive force (PAF) representing  
272 maximum force required to separate the films from the simulated wound surface, the area under  
273 the curve (AUC) representing the total work of adhesion (TWA) and the cohesiveness

274 representing the distance travelled (mm) before detaching from the simulated wound surface  
275 were determined.

276

## 277 2.10 In vitro protein dissolution and release studies

278 The in vitro protein dissolution and release studies were carried out as previously described  
279 [22]. A modified Franz diffusion cell with a wire mesh washed by 8mL SWF (pH 7.5, 37°C)  
280 was used to simulate the natural wound environment. The protein (6.6mg/g) loaded film  
281 dressings (50mg, n=4) were placed on the wire mesh. Aliquots (200µL) of SWF was withdrawn  
282 at regular intervals and analyzed using Bradford assay and replaced with same volume of fresh  
283 SWF (pH 7.5) to maintain a constant volume and sink conditions. The absorbance of the  
284 sampled aliquot was measured using a Multi-scan EX Micro-plate photometer (Thermo  
285 Scientific, Essex, UK) at 595nm and 450nm and the ratio of the absorbance values determined  
286 (from linearization of the curve as described in [23, 24]. The cumulative percentage (%) drug  
287 release was plotted against time and the proteins release kinetics determined by finding the best  
288 fit of the % release against time data to Higuchi (equation 5), Korsmeyer-Peppas (equation 6),  
289 zero order (equation 7) and first order (equation 8) equations.

290

$$291 \quad Q_t = k_H t^{1/2} \quad \text{Equation 5}$$

292  $Q_t$  is the amount of drug released at time (t),  $k_H$  is the (Higuchian) release rate constant.

293

$$294 \quad \ln(Q_t / Q_\infty) = \ln k + n \ln t \quad \text{Equation 6}$$

295  $Q_t$  is the amount of drug released at a given time (t),  $Q_\infty$  is the amount of drug present initially,  
296 k is a constant involving the geometry and structural characteristics of the film and n release  
297 exponent.

298

$$299 \quad Q_t - Q_0 = k_0 t \quad \text{Equation 7}$$

300  $Q_t$  is the amount of drug released in time (t),  $Q_0$  is the amount of drug dissolved at time zero  
301 and  $k_0$  is the zero-order release rate constant.

302

$$303 \quad \ln(Q_{\infty} / Q_1) = k_1 t \quad \text{Equation 8}$$

304  $Q_{\infty}$  is the initial total amount of drug present,  $Q_1$  is the amount of remaining drug at time (t) and

305  $k_1$  is the first order release rate constant.

306

### 307 2.11 Far-UV circular dichroism spectroscopy

308 The conformational (secondary) structures of the pure model proteins (GST-GFP, GST and  
309 GFP) and released protein from the films dressings were examined in the far-UV region of a  
310 circular dichroism (CD) instrument; wavelength range (190–260nm), band width (1nm), path  
311 length (0.01cm) and 10 seconds time per point, in 0.01M PBS (pH 7.5) at 20°C using a  
312 Chirascan CD spectrometer (Chirascan, Applied Photophysics, UK).

313

### 314 2.12 Statistical analysis

315 The various formulations and experimental variables used to characterize the films were  
316 compared by statistical data evaluation (Microsoft Excel, Office 2013 software) using a two  
317 tailed student t-test at 95% confidence interval (p-value < 0.05) as the minimal level of  
318 significance.

319

320

## 321 **3 Results**

### 322 3.1. Protein characterization

323 The molecular weights of the proteins observed on the gel were 52kDa, 27kDa and 28kDa  
324 confirming the proteins of interest i.e. GST-GFP, GFP and GST (pGEX3x and pGEX5x)  
325 respectively. The molecular weights observed from immune-blotting: GFP (27 kDa), GST (28  
326 kDa) and GST-GFP (52kDa), shown in Fig. 1a, 1b and 1c respectively, correspond to that  
327 reported in the literature [19] and confirmed the Coomassie observations.

328

### 329 3.2 MTT cytotoxicity assay

330 Fig. 2 shows the toxicity profile for dextran and PEI, GST-GFP, GST, GFP and SA respectively  
331 (n = 6). The results showed 5-10% cell viability for PEI with cell death at 72 hours and 100%  
332 cell viability for dextran as was expected. Almost 100% cell viability was observed for GST-  
333 GFP, GST, GFP and SA after 72 hours, with negligible cell death noticed and therefore, all  
334 three proteins and SA were confirmed as non-toxic. The results (Fig. 2F) show a clear profile  
335 of the cytotoxicity of SA on adherent epithelial mammalian cells (Vero (ATCC<sup>®</sup> CCL-81<sup>™</sup>)  
336 confirming that SA is non-toxic under the conditions tested. This is not surprising since SA is  
337 approved for oral formulations and moist wound dressings and therefore the results here  
338 confirm its safety for use as a protein delivery dressing for wound healing.

339

### 340 3.3 Thermal analysis

#### 341 3.3.1 High sensitivity differential scanning calorimetry (HSDSC)

342 Table 1 shows the HSDSC profiles of the three proteins obtained by varying three main  
343 experimental conditions (scan rate, pH and concentration). Detailed description of the results  
344 showing the effect of the three experimental variables on the HSDSC profiles are provided as  
345 supplementary data in appendix A1.

#### 346 3.3.2 Differential scanning calorimetry (DSC)

347 All three proteins showed similar characteristics as observed in their thermograms (Fig. 3A).  
348 Detailed descriptions of the DSC results for the pure proteins are given in appendix A2. GLY  
349 showed two endothermic peaks at 136.54°C and 293.67°C attributed to water loss and boiling  
350 (Fig. 3B) whilst SA showed one endothermic peak at 109.23°C and an exothermic peak at  
351 242.59°C (Fig. 3C) that can be attributed to dehydration and thermal degradation of  
352 intermolecular side chains respectively [26, 27]. Differences were observed between the DSC

353 thermograms of the blank and protein loaded films (Fig. 3D) which could be an indication of  
354 interaction between the polymer and proteins. The blank film was characterized by two  
355 endothermic transitions at 98.61°C and 250.05°C (Fig. 3D). However, the protein loaded films  
356 showed four endothermic transitions with multiple stages of polymer degradation with the  
357 exception of GST (30.2, 3.3mg/g) and GST-GFP (30.2mg/g) respectively, which showed two  
358 endothermic transitions (Fig. 3D). The high dehydration temperatures seen in both blank and  
359 protein loaded films with endset peak at 126.32°C can be attributed to bound water molecules  
360 within the polymeric film allowing for more hydrophobic interactions between protein  
361 molecules.

362

### 363 3.3.3 Thermogravimetric analysis (TGA)

364 Table 2 shows the different (1<sup>st</sup> – 4<sup>th</sup>) thermal events and the dynamic weight loss associated  
365 with those events. In all cases, the first dynamic weight loss observed can be attributed to  
366 desorption of water hydrogen bonded to the polymer structure [28]. SA powder had higher  
367 moisture content (18.24%) than the films (6.52-16.68%) which could be attributed to the drying  
368 process employed when formulating the films. The peak temperature at which the moisture  
369 content within the blank film matrix was lost was significantly lower (45.1°C) than those of  
370 the protein loaded films. This bonded water can be clearly seen in all protein loaded film  
371 temperatures ranging from 53.9°C to 112.2°C. The degradation temperatures decreased for all  
372 the films in comparison to the starting material (SA). This can be attributed to the effect of the  
373 formulation process in changing the physiochemical properties of the starting material due to  
374 interactions between the components of the formulation. SA showed a three stage degradation  
375 process (236.7°C, 257.6°C and 388.7°C) that can be attributed to the presence of carbonaceous  
376 residues [29]. However, GLY only showed one main thermal event above 200°C at a  
377 temperature of 220.4°C which might relate to boiling as observed in DSC, though the

378 temperatures are different. This shows that the starting materials (SA and GLY) are thermally  
379 stable up to temperatures above 200°C.

380

### 381 3.4 Mechanical tensile characterization

382 Table 3A shows that unplasticised films (SA:GLY 1:0) were highly brittle as evidenced by  
383 having the lowest % elongation ( $1.85 \pm 0.19\%$ ) and highest values for both elastic modulus and  
384 tensile strength, implying these could cause trauma to newly formed skin cells on a healing  
385 wound [15]. However, addition of GLY caused a general increase in flexibility as evidenced  
386 by the increased % elongation (from 1.85 to 38.84%) and decrease in both Young's modulus  
387 (rigidity) (from 20.77 to 0.40mPa) and tensile strength (brittleness) (from 51.34 to 6.12  
388 N/mm<sup>2</sup>). This can be attributed to GLY interpolating itself between SA polymer chains  
389 resulting in reduced interaction and the intermolecular cohesive forces between the polymer  
390 chains [30, 31].

391

392 Table 3B shows the variations in tensile profiles based on the type and amount of protein for  
393 the optimized films (SA:GLY 1:2). The % elongation at break reduced from  $38.84 \pm 0.86\%$  for  
394 blank films to between  $23.31 \pm 4.04$  and  $5.46 \pm 0.92\%$  depending on the type and amount of  
395 protein loaded. These values are below that considered ideal for wound dressing as it suggests  
396 lower elasticity. However, the elastic (Young's) modulus and tensile strength values showed  
397 the films were not too brittle and this was confirmed during physical handling of the drug  
398 loaded films. Further, the three different protein loaded films possessed different levels of  
399 flexibility with GST-GFP films having the highest flexibility (highest % elongation) as  
400 opposed to GST and GFP loaded films. This could be as a result of GST-GFP being a construct  
401 of both proteins, therefore an increase in molecular weight.

402

403 From the results in Table 3, it can be seen that on the whole, Young's modulus decreased with  
404 increasing concentrations of proteins with the exception of GFP where the value increased from  
405  $0.97 \pm 0.40\text{mPa}$  for 3.3mg/g film to  $2.14 \pm 0.34\text{mPa}$  for 6.6mg/g film but then decreased to  
406  $0.88 \pm 0.17\text{mPa}$  for the 30.2mg/g film. This suggests that the protein incorporated in the films  
407 improved the films toughness and ability to withstand mechanical pressure whilst maintaining  
408 enough flexibility. Generally, a decrease in tensile strength was observed for most of the  
409 protein loaded films (except GFP 6.6mg/g and GST 3.3mg/g films) in comparison to the blank  
410 films, implying a reduction in film brittleness. This suggests that the proteins possess some  
411 degree of plasticizing effect on the films, thereby imparting flexibility, elasticity and improved  
412 toughness.

413

### 414 3.5 Scanning electron microscopy (SEM)

415 Fig. 4 shows that increasing GLY (plasticizer) concentration had an effect on the film  
416 morphology. The unplasticised film showed a clear uniform morphology whilst films prepared  
417 from gels containing SA:GLY 2:1, 4:3, 1:1 showed a rough uneven topography. Furthermore,  
418 it can be seen from Fig. 4 that with further increase in the concentration of GLY in the original  
419 gel (SA:GLY 2:3, 1:2), the topography of the films smoothens out, therefore producing  
420 homogenous uniform films that will be suitable for protein loading. SA film containing GLY  
421 in ratio SA:GLY 1:2, was chosen as being the most uniform of the six formulated films (Fig.  
422 4) and used for protein loading, which confirms the tensile results.

423

424 The proteins (GFP, GST and GST-GFP) had little impact on the film morphology and  
425 topography (Fig. 5) of the optimized films though slight differences could be observed between  
426 GFP, GST and GFP-GST loaded films based on the drug loading, GFP, GST and GST-GFP  
427 (Fig. 5 A, D and G) respectively.

### 428 3.6 Hydration and swelling

429 It can be observed from Fig. 6 that most of the films showed percentage swelling index values  
430 ranging from approximately 650 to 1000% which were not significant ( $p > 0.05$ ) as evidenced  
431 by the positions of the standard deviation bars. However, two films with higher concentrations  
432 (30.2mg/g) of GST-GFP, and GFP) possessed significantly ( $p < 0.05$ ) higher percentage  
433 swelling index values compared to the other drug loaded films. The higher percentage swelling  
434 index observed in the higher protein (30.2 mg/g) loaded films could be attributed to the high  
435 protein content attracting water molecules due to its increased solubility. Both blank and  
436 protein loaded films showed high percentage swelling index, indicating a high holding capacity  
437 for wound exudate while still maintaining their structural integrity which can be attributed to  
438 hydrogel properties of SA.

439

### 440 3.7 In-vitro wound adhesion

441 The peak adhesive force (PAF) representing maximum force required to separate the films  
442 from the simulated wound surface, the area under the curve (AUC) representing the total work  
443 of adhesion (TWA) and the cohesiveness representing the distance travelled (mm) before  
444 detaching from the simulated wound surface were determined. Fig. 7 showed that the blank  
445 films had the highest cohesiveness and TWA values with the latter indicating the strong  
446 interactions (hydrogen bond formation) between the polymeric chains of SA and the simulated  
447 wound surface. There was no statistically significant difference observed in PAF (stickiness)  
448 between the GFP loaded films and the blank film ( $p = 0.7132, 0.0610, 0.7703$  respectively).  
449 However, there was significant differences observed in TWA between the blank and GFP  
450 loaded films ( $p = 0.0045, 0.0010, 0.0022$  respectively). In addition, GFP loaded films  
451 containing 30.2mg/g, 6.6mg/g of the protein showed no significant difference in cohesiveness

452 with the blank films ( $p = 0.0807, 0.1375$ ) while GFP loaded film containing 3.3mg/g of the  
453 protein was significantly different from the blank film in cohesiveness ( $p = 0.0211$ ).

454

455 Generally, it was also noted (Fig. 7) that with decrease in protein concentration, an increase in  
456 adhesive strength (TWA and PAF) was observed for all protein loaded films. This could be the  
457 result of higher protein loading (30.2mg/g) impacting on the films, providing less free hydrogen  
458 bonding sites leading to higher hydration as seen in Fig. 7 and less adhesive strength.

### 459 3.8 In vitro protein dissolution and release studies

460 Fig. 8 shows that the film dressings appeared to show rapid initial release of protein followed  
461 by constant release over a longer period. However, GST loaded dressing showed higher total  
462 cumulative release (90%) than GFP (78%) and GST-GFP (67%) dressings. It can also be seen  
463 that 78%, 70% and 64% release from GST, GFP and GST-GFP loaded dressing films  
464 respectively occurred within the first 2 hours (Fig. 8 inset). According to Table 4, GST-GFP  
465 protein release was proportional to time which is a non-concentration dependent mechanism  
466 involving the swelling and dissolution of the polymeric matrix (zero order mechanism). GFP  
467 released was proportional to the square root of time ( $t^{1/2}$ ) indicating a Fickian diffusion  
468 controlled mechanism. GST however, had identical  $R^2$  values for both Higuchi and zero order  
469 mechanisms. Therefore, GST release data was further evaluated using the Korsmeyer-Peppas  
470 equation and the diffusional exponent ( $n$ ) was determined to be less than 0.5 ( $n < 0.5$ ) indicating  
471 a quasi-Fickian diffusion mechanism [32].

472

### 473 3.9 Structural stability of model proteins by far-UV CD spectroscopy

474 Fig. 9A, B and C show the far-UV spectra of GST-GFP, GST and GFP in their native state  
475 (control) and after release from the SA film dressings (post-formulation). The ratios of the  
476 mean residue ellipticity were calculated as previously described. The two maxima bands

477 observed at 209 and 222nm [33, 34] were respectively assigned to the  $\alpha$ -helical and  $\beta$ -sheet  
478 structures of GST-GFP (Fig. 9A) and GST (Fig. 9B). GST-GFP and GST released from SA  
479 films and the native protein showed similar mean residue ellipticity ratios ( $\theta_{209} / \theta_{222}$ ) of 1.0  
480 (GST-GFP) and 1.2 (GST). Fig. 9C (GFP) shows that GFP predominantly consisted of  $\beta$ -sheet  
481 structures and has also been reported by Visser and co-workers [35]. The similarity in the far-  
482 UV spectra (Fig. 9A, B and C) and the mean residue ellipticity ratios obtained (GST-GFP and  
483 GST) pre and post-formulation confirmed the conformational stability of all three proteins  
484 within the film dressings.

485

#### 486 **4. Discussion**

487 The model proteins (GST, GFP and GST-GFP) were chosen because they could be readily  
488 cultured using bacteria (in house), isolated and characterized with various physical and bio-  
489 analytical techniques. This was necessary due to the large amounts of proteins needed during  
490 the formulation development and optimization process. Coomassie staining was used to detect  
491 the molecular weights of the recombinant GST-GFP protein and BSA at concentrations 5 $\mu$ g  
492 and 75 $\mu$ g respectively. BSA was used as a control to validate that the gel was working  
493 optimally as its molecular weight is constant (~66kDa) and confirmed that the proteins were  
494 separated according to molecular weight.

495

496 All the materials used were generally considered as safe (GRAS). Dextran (synthesized by  
497 *Leuconostoc* bacteria) is a complex polysaccharide made of glucose molecules [36] and was  
498 used as a negative control due to its low toxicity. On the other hand, PEI is a commercially  
499 available polyamine [37] and a gene carrier with reasonable transfection efficiency and high  
500 cytotoxicity. It is reported in literature [38, 39] that SA is generally regarded as non-toxic and  
501 used in oral formulations as well as food substances, however, none of these literature

502 references show a clear profile on the absence of toxicity of SA against epithelial cells. In the  
503 current study, safe model proteins have been used but this test can also be used in  
504 determining toxicity levels of growth factors (which play an important role during wound  
505 healing) on live mammalian epithelial cells. This will help to investigate the effect of  
506 different dose levels of growth factors delivered directly to wound sites, to avoid excessive  
507 proliferation of cells and thus, preventing the risk of triggering cancerous cells.

508

509 The stability of the proteins under various conditions were investigated using various thermal  
510 analysis techniques. Though two related scanning calorimetry techniques (HSDSC and DSC)  
511 were used, this was necessary since the HSDSC is effective for analyzing sensitive biological  
512 samples such as proteins as well as liquid samples (solutions) whilst DSC is generally more  
513 useful for samples in the solid state and small molecules. The HSDSC data shows that the  
514 GFP is a more thermally stable protein than GST. Therefore high temperatures of up to 70°C  
515 (14°C less than the  $T_{max}$  of GFP at pH 7.5) and temperatures of up to 45°C (14°C less than  
516 the  $T_{max}$  of GST at pH 7.5) can be employed during formulation or processing. The ratio  
517  $T_m/T_{max}$  is an indicator of thermal stability and generally, the higher the  $T_m/T_{max}$ , the more  
518 thermodynamically stable the protein [25]. Generally, the variations observed in the HSDSC  
519 can be attributed to the influence of pH, causing aggregation and / or degradation of the  
520 proteins within the buffers at the various pH values especially at 6.0 and 10.0.

521

522 DSC was used to determine possible interactions between the various film components as well  
523 as stability of the proteins within the film matrix. The exothermic peak observed in SA was not  
524 seen in the formulated gels or in the films possibly due to interactions between the formulation  
525 components, and molecular dispersion of the protein drugs within the formulation [40]. This  
526 observation is similar to that previously reported in another study [41] where degradation

527 exotherm of pure SA was absent in corresponding drug loaded alginate beads but rather, an  
528 endotherm, corresponding to the interaction of alginate with calcium ions naturally present in  
529 SA was observed. The differences observed between the DSC profiles could be an indication  
530 of fewer interactions between the GST proteins (3.3 and 30.2mg/g) and the polymer network  
531 and further evidenced by the closeness of the dehydration peak temperatures and enthalpies for  
532 GST (3.3 and 30.2mg/g) loaded and blank films.

533

534 The TGA results demonstrate that the different films generally possessed similar water content.  
535 The higher temperature of complete water loss in protein loaded films could be related to  
536 intermolecular forces such as hydrogen-bonds, van der Waals force and hydrophobic  
537 interactions between the proteins, and the starting materials within the film matrix, resulting in  
538 well-ordered bound water compared to the free water in the blank films. It is reported that water  
539 molecules play a vital role in maintaining the structure, dynamics, stability and function of  
540 biological molecules as they are responsible for packing and stabilization of the protein  
541 structure particularly in forming H-bond networks and screening of electrostatic interactions  
542 [42]. Papoian et al., reported a substantial improvement in protein structure prediction by  
543 adding a water-based potential to a well-known Hamiltonian for protein structure prediction  
544 [43]. Wetting the Hamiltonian improved the predicted structures, particularly of large proteins  
545 (>115 amino acid residues) through long range interactions between charged or polar groups  
546 facilitated by water molecules. However, bulk free water allows for rotational freedom within  
547 proteins, causing flexibility and enzymatic activities, thus, increasing reactivity and therefore  
548 an increase in entropy (disorderliness) in the protein [44].

549

550 Overall, the thermal analysis data shows the impact of the dressing formulation on the  
551 properties of the protein and vice versa in terms of stability and mechanical integrity

552 respectively. At the temperature of 45°C and 40°C used for gel preparation and oven drying  
553 respectively, it is feasible to undertake the formulation development of alginate based  
554 dressing incorporating therapeutically relevant macromolecules without causing degradation.  
555 However, this will need to be confirmed with actual therapeutic proteins such as growth  
556 factors.

557

558 Texture analysis was used to measure the tensile properties; first to determine the effect of  
559 GLY concentrations the film behavior and the resulting data used to select the most appropriate  
560 formulation for protein loading and determine effect of drug concentration on the film tensile  
561 properties. Generally for film dressings, a balance between toughness (rigidity) and elasticity  
562 (flexibility) is required [15]. Tough films allow ease of handling without being sticky and  
563 folding up, whilst being flexible enough to allow easy application to the wound site and enable  
564 applications to difficult areas of the body such as parts around the joints and under the foot.  
565 This is normally achieved by having a % elongation value between 30–60% [15, 40] and this  
566 was only satisfied by the SA:GLY 1:2 films with % elongation value of 38.84% and were  
567 therefore selected for drug loading and further testing.

568

569 The rough and uneven topography (SEM) observed in films prepared from gels containing  
570 SA:GLY 2:1, 4:3, 1:1, can be detrimental to protein loading as content uniformity cannot be  
571 achieved in these films due to their rough topography. Rather, loaded drugs could be trapped  
572 and non-uniformly dispersed across the rough surfaces of these films, thereby hindering dosage  
573 accuracy as well as consistent drug release.

574

575 For effective wound healing, an ideal dressings is expected to be able to absorb large quantities  
576 of exudate whilst maintaining its structural integrity over long periods as well as keeping the

577 wound environment moist to facilitate wound healing. SA dressings are good absorbents that  
578 gradually form hydrophilic gels upon contact with wound exudate, thereby promoting a moist  
579 wound environment, the formation of granulation tissue and wound healing. It is reported [2]  
580 that moderate to high exuding wounds produce approximately 3-5 mL of wound exudate /  
581 10 cm<sup>2</sup> in 24 hours. Therefore, 0.6-1.0 mL wound exudate is produced per 2 cm<sup>2</sup> in 24 hours.  
582 In this study, films (blank and protein loaded) absorbed 625-1732% of SWF which is an  
583 indication that these dressings can absorb high amounts of wound exudate and can be used for  
584 moderate to high exuding wounds. It is reported that excessive hydrations as seen in the higher  
585 protein loaded films (30.2mg/g) (Fig. 6) can lead to reduced bioadhesion due to the formation  
586 of a slippery surface between the films and the simulated wound surface [45]. Adhesivity in  
587 wound healing is important as wound dressing should be self-adhesive with the wound so as  
588 not to fall off but be easily removed and painless [7].

589

590 Furthermore, the higher swelling properties of the 30.2mg/g protein loaded films could have  
591 led to a reduction in flexibility, which is important as it determines the extent of entanglement  
592 and enhances interpenetration between polymer (SA) and the simulated wound surface. The  
593 comparison of the swelling and bio-adhesive properties of the different formulations was used  
594 to determine the film dressing with the ideal functional properties. Based on the observed  
595 profiles, the 6.6mg / g protein loaded film was concluded to be the dressing with the optimum  
596 swelling and bio-adhesive properties and was subsequently used for in vitro drug (protein)  
597 dissolution studies.

598

599 The differences observed in the overall % cumulative release might relate to the relative  
600 difference in solubility between the three proteins as well as their interactions with the polymer  
601 (SA). In addition, initial burst release may be attributed to the dissolution and rapid release of

602 the surface associated protein molecules coupled with initial hydration and swelling above 60%  
603 in the first hour. Generally for a polymeric matrix such as solvent cast films, swelling, and  
604 solute diffusion and matrix degradation are proposed as the main driving forces responsible for  
605 drug release [46, 47]. Overall, it can be seen (Fig. 8) that after the initial burst release, the  
606 protein release was sustained over a period of 72 hours for all three protein loaded films. This  
607 second phase could be attributed to diffusion from the hydrated and swollen gel. This will help  
608 prevent frequent changing of the dressings so as not to disrupt newly formed skin tissues,  
609 reduce side effects through extended dosing as well as for patient compliance [46].

610

## 611 **5 Conclusions**

612 Adhesive SA film dressings were successfully developed as potential protein delivery systems  
613 for wound healing. The blank (SA:GLY 1:2) film was determined to be the optimized  
614 formulation for protein drug loading and further development. The absence of free water  
615 molecules within the film matrix was advantageous to ensure protein stability in the film and  
616 was confirmed by CD. Overall, the formulations containing 6.6mg of protein per gram of film  
617 exhibited optimum hydration and adhesive properties required for wound dressings. Further,  
618 protein release from the dressing was sustained over 72 hours which is expected to allow good  
619 bioavailability of the model protein drug at the site of action.

620

## 621 **6. Conflict of interest**

622 The authors report no conflict of interest

623

## 624 **7. References**

- 625 1. F. Strodtbeck, Physiology of Wound Healing. Newborn Infant Nurs. Rev. 1(0) (2001)  
626 43–52.

- 627 2. J.S. Boateng, H.V. Pawar, J. Tetteh, Polyox and carrageenan based composite film  
628 dressing containing anti-microbial and anti-inflammatory drugs for effective wound  
629 healing. *Int. J. Pharm.* 441 (2013) 181– 191.
- 630 3. C. Stephanie, W.M. Wu, D.G. Armstrong, Wound care: The role of advanced wound  
631 healing technologies. *J. Vasc. Surg.* 52(3) (2010) 59S-66S.
- 632 4. S. Enoch, K. Harding, Wound Bed Preparation: The Science Behind the Removal of  
633 Barriers to Healing. *Wounds.* 15 (7) 2003.
- 634 5. V. Falanga, Wound healing and its impairment in the diabetic foot. *Lancet.* 366 (2005)  
635 1736–1743.
- 636 6. P.S. Murphy, G.R.D. Evans, Advances in Wound Healing: A Review of Current Wound  
637 Healing Products. *Plast. Surg. Int.* Vol 2012; Article ID 190436, (2012) 8 pages.  
638 doi:10.1155/2012/190436.
- 639 7. J.S. Boateng, K.H. Matthews, H.N.E. Stevens, G.M. Eccleston, Wound Healing  
640 Dressings and Drug Delivery Systems: A Review. *J. Pharm. Sci.* 97(8) (2008) 2892-  
641 2923.
- 642 8. S.A.L. Bennett, H.C. Birnboim, Receptor-mediated and protein kinase-dependent  
643 growth enhancement of primary human fibroblasts by platelet activating factor. *Mol.*  
644 *Carcinog.* 20(4) (1997) 366–375.
- 645 9. P. Zahedi, I. Rezaeian, S.O. Ranaei-Siadat, S.H. Jafari, P. Supaphol, A review on  
646 wound dressings with an emphasis on electrospun nanofibrous polymeric bandages.  
647 *Polym. Adv. Technol.* 21 (2010) 77–95.
- 648 10. P.M. Jarvis, D.A.J. Galvin, S.D. Blair, How does calcium alginate achieve hemostasis  
649 in surgery? *Proceedings of the 11th Congress on Thrombosis and Hemostasis.* 58  
650 (1987) 50.

- 651 11. F. Collins, S. Hampton, R. White, A-Z Dictionary of Wound Care 2002. Dinton,  
652 Wiltshire: Mark Allen Publishing Ltd.
- 653 12. S.D. Blair, P. Jarvis, M. Salmon, C. McCollum, Clinical trial of calcium alginate  
654 hemostatic swabs. *Br. J. Surg.* 77 (1990) 568–570.
- 655 13. S.D. Blair, C.M. Backhouse, R. Harper, J. Matthews, C.N. McCollum, Comparison of  
656 absorbable materials for surgical hemostasis. *Br. J. Surg.* 75 (1988) 69–71.
- 657 14. A. Thomas, K.G. Harding, K. Moore, Alginates from wound dressings activate human  
658 macrophages to secrete tumor necrosis factor- $\alpha$ . *J. Biomater.* 21 (2000) 1797–1802.
- 659 15. J.S. Boateng, K.H. Matthews, A.D. Auffret, M.J. Humphrey, H.N. Stevens, G.M.  
660 Eccleston, In vitro drug release studies of polymeric freeze-dried wafers and solvent-  
661 cast films using paracetamol as a model soluble drug. *Int. J. Pharm.* 378 (2009) 66–72.
- 662 16. T. Gilchrist, A.M. Martin, Wound treatment with Sorbsan - An alginate fiber dressing.  
663 *Biomater.* 4 (1983) 317–320.
- 664 17. M.S. Agren, Four alginate dressings in the treatment of partial thickness wounds: A  
665 comparative study. *J. Plast. Surg.* 49 (1996) 129–134.
- 666 18. D.A. Morgan, Wounds-What should a dressing formulary include? *Hosp. Pharm.* 9  
667 (2002) 261-266.
- 668 19. M.W. Pettit, P.D. Dyer, J.C. Mitchell, P.C. Griffiths, B. Alexander, B. Cattoz, R.K.  
669 Heenan, S.M. King, R. Schweins, F. Pullen, S.R. Wicks, S.C. Richardson, Construction  
670 and physiochemical characterization of a multi-composite, potential oral vaccine  
671 delivery system (VDS). *Int. J. Pharm.* 468 (2014) 264-271.
- 672 20. J.F. Urbanowski, R.C. Piper, The Iron Transporter Fth1p Forms a Complex with the  
673 Fet5 Iron Oxidase and Resides on the Vacuolar Membrane. *J. Bio. Chem.* 274(53)  
674 (1999) 38061–38070.

- 675 21. G. Gethin, The significance of surface pH in chronic wounds. *Wounds UK*. 3(3)  
676 (2007) 52–56.
- 677 22. H.V. Pawar, J.S. Boateng, I. Ayensu, J. Tetteh, Multi functional medicated  
678 lyophilized wafer dressing for effective chronic wound healing. *J. Pharm. Sci.* 103(6)  
679 (2014) 1720-1733.
- 680 23. O. Ernst, T. Zor, Linearization of the Bradford Protein Assay. *J. Vis. Exp.* 38 (2010) 1-  
681 7.
- 682 24. T. Zor, Z. Selinger, Linearization of the Bradford Protein Assay Increases its  
683 sensitivity: Theoretical and Experiment Studies. *Anal. Biochem.* 236 (1996) 302-308.
- 684 25. G. Bruylants, J. Wouters, C. Michaux, Differential Scanning Calorimetry in life  
685 sciences: thermodynamics, stability, molecular recognition and applications in drug  
686 design. *Curr. Med. Chem.* 12 (2005) 2011-2020.
- 687 26. J.P. Soares, J.E. Santos, G.O. Chierice, E.T.G. Cavalheiro, Thermal behavior of alginic  
688 acid and its sodium salt. *Eclet. Quim.* 29(2) (2004) 57-62.
- 689 27. C. Xiao, Y. Lu, H. Liu, L. Zhang, Preparation and physical properties of blend films  
690 from sodium alginate and polyacrylamide solutions. *Macromol. Sci. Pure Appl. Chem.*  
691 A37(12) (2000) 1663–1675.
- 692 28. M.J. Zohuriaan, F. Shokrolahi, Thermal studies on natural and modified gums. *Polym.*  
693 *Test.* 23 (2004) 575-579.
- 694 29. C. Giovino, J. Tetteh, J.S. Boateng, 2012. Development and characterization of  
695 chitosan films impregnated with insulin loaded PEG-b-PLA nanoparticles (NPs): A  
696 potential approach for buccal delivery of macromolecules. *Int. J. Pharm.* 428: 143–151.
- 697 30. C. Giovino, I. Ayensu, J. Tetteh, J.S. Boateng, An integrated buccal delivery system  
698 combining chitosan films impregnated with peptide loaded PEG-b-PLA nanoparticles.  
699 *Coll. Surf. B: Biointerf.* 112 (2013) 9-15.

- 700 31. A. Sajid, S. Swati, K. Awdhesh, S. Sant, T. Ansari, G. Pattnaik, Preparation and In-  
701 Vitro Evaluation of sustained release matrix tablets of phenytoin sodium using natural  
702 polymers. *Int. J. Pharm. Pharmacol. Sci.* 2(3) (2010) 174-179.
- 703 32. I. Ayensu, J.S. Boateng, Development and Evaluation of Lyophilized Thiolated  
704 Chitosan Waters for buccal delivery of proteins. *J. Sci. Tech.* 32(2) (2012) 46-55.
- 705 33. I. Ayensu, J.C. Mitchell, J.S. Boateng, In-vitro characterization of thiolated chitosan  
706 based lyophilized formulations for buccal mucosa delivery of proteins. *Carb. Polym.*  
707 89 (2012) 935-941.
- 708 34. N.V. Visser, M.A. Hink, J.W. Borst, G.N.M. van der Krogt, A.J.W.G. Visser, Circular  
709 dichroism spectroscopy of fluorescent proteins. *FEBS Lett.* 521 (2002) 31-35.
- 710 35. J. Maia, A.C. Rui, F.J. Jorge, P.N. Coelho, M. Simões, G. Helena, Insight on the  
711 periodate oxidation of dextran and its structural vicissitudes. *Polym.* 52 (2) (2011) 258-  
712 265.
- 713 36. L. Hongtao, Z. Shubiao, W. Bing, C. Shaohui, Y. Jie, Toxicity of cationic lipids and  
714 cationic polymers in gene delivery. *J. Contr. Rel.* 114 (2006) 100–109.
- 715 37. M. George, T.E. Abraham, Polyionic hydrocolloids for the intestinal delivery of protein  
716 drugs: Alginate and chitosan: a review. *J. Contr. Rel.* 114 (2006) 1–14.
- 717 38. T. Andersen, B.L. Strand, K. Formo, E. Alsberg, Alginates as biomaterials in tissue  
718 Engineering. *Carbohydr. Chem.* 37 (2012) 227-258.
- 719 39. A. Ganem-Quintanar, M. Silva-Alvarez, R. Alvarez-Román, N. Casas-Alancaster, J.  
720 Cázares-Delgadillo, D. Quintanar-Guerrero, Design and evaluation of a self-adhesive  
721 naproxen-loaded film prepared from a nanoparticle dispersion. *J. Nanosci.*  
722 *Nanotechnol.* 6(9-10) (2006) 3235-41.
- 723 40. A. Rajendran, Sanat Kumar Basu SK Alginate-Chitosan Particulate System for  
724 Sustained Release of Nimodipine. *Trop. J. Pharm. Res.* 8(5) (2009) 433-440.

- 725 41. Y. Levy, J.N. Onuchic, Water and proteins: A love-hate relationship. PNAS 101(10)  
726 (2004) 3325–3326.
- 727 42. G.A. Papoian, J. Ulander, M.P. Eastwood, Z. Luthey-Schulten, P.G. Wolynes, Water  
728 in protein structure prediction. PNAS. 101(10) (2004) 3352–3357.
- 729 43. D. Lucent, C.D. Snow, C.E. Aitken, V.S. Pande, Non-Bulk-Like Solvent Behavior in  
730 the Ribosome Exit Tunnel. PLoS Comput. Biol. 6(10) (2010) e1000963.  
731 doi:10.1371/journal.pcbi.1000963.
- 732 44. B. Phanindra, B.K. Moorthy, M. Muthukumaran, Recent Advances in  
733 Mucoadhesive/Bioadhesive Drug Delivery System: A Review. Int. J. Pharm. Med. Bio.  
734 Sci. 2(1) (2013) 68-84.
- 735 45. Y. Fu, W.J. Kao, Drug Release Kinetics and Transport Mechanisms of Nondegradable  
736 and Degradable Polymeric Delivery Systems. Exp. Opin. Drug Deliv. 7(4): (2010) 429–  
737 444. doi:10.1517/17425241003602259.
- 738 46. H. Pawar, J. Tetteh, J.S. Boateng, Preparation and characterization of novel wound  
739 healing film dressings loaded with streptomycin and diclofenac. Coll. Surf. B:  
740 Biointerf. 102 (2013) 102–110.
- 741 47. J.S. Boateng, R. Burgos-Amardo, O. Okeke, H. Pawar, Development, optimization and  
742 functional characterization of freeze-dried wafers containing silver sulfadiazine for  
743 wound healing. Int J Biol Macromol. 79 (2015) 63-71.
- 744
- 745
- 746
- 747

748 **Figure Legends**

749 Fig. 1. (a) Developed X-ray film showing detection of affinity purified GFP by western  
750 immunoblotting (anti body dilutions, 1:3000, exposure time; 10 seconds); (b) developed X-ray  
751 film showing detection of affinity purified GST by western immunoblotting (anti body  
752 dilutions, 1:3000, exposure time; 10 seconds) and (c) developed X-ray film showing detection  
753 of affinity purified recombinant GST-GFP by western immunoblotting (anti body dilutions,  
754 1:2000, exposure time; 1 second).

755

756 Fig. 2. Toxicity profiles of SA (starting material), dextran and PEI used as negative and positive  
757 controls respectively ( $n=6 \pm SD$ ), the three model protein drugs (GST, GFP and GST-GFP)  
758 ( $n=6 \pm SD$ ) against vero cell lines after 72 hours exposure time.

759

760 Fig. 3. DSC thermograms of (A) GLY, (B) SA and (C) the blank and protein loaded films.

761

762 Fig. 4. SEM micrographs (x50 magnification) showing the effect of increasing GLY  
763 concentrations on film topography and morphology.

764

765 Fig. 5. SEM micrographs (x200 magnification) showing the effect of protein loading on the  
766 surface morphological properties of the plasticized SA: GLY (1:2) films containing [GFP (A-  
767 C), GST, (D-F) and GST-GFP (G-I) loaded film from high (left) to low (right) concentrations  
768 (30.2, 6.6 and 3.3mg/g) respectively.

769

770 Fig. 6. Hydration and swelling profiles of the blank and protein loaded film dressings ( $n=3 \pm$   
771 SD).

772

773 Fig. 7. In vitro adhesive profiles for blank and drug loaded films ( $n=4 \pm SD$ )

774

775 Fig. 8. Dissolution profiles of protein (6.6mg/g) loaded film dressings ( $n = 4, \pm SD$ )

776

777 Fig. 9. CD spectra of (A), GST-GFP, (B), GST and (C), GFP in native state and post release  
778 from film dressing (0.96mg/mL solution used).

779

780

781

782

783

784

785

786

787

788

789

790

791

792

793

794

795

796

797

798 **TABLES**

799 Table 1

800 Thermal stability of proteins (GST-GFP, GST and GFP) as a function of scan rate,  
 801 concentration and pH using HSDSC.

<b>Protein</b>	<b>Scan rate (°C/min)</b>	<b>Concentration (mg/mL)</b>	<b>ΔH (KJ/mol)</b>	<b>T<sub>max</sub> (°C)</b>	<b>pH</b>		
GST	0.5	5.0	73.25	56.27	7.5		
GST	1.0	5.0	91.35	57.77	7.5		
GST	2.0	5.0	66.14	59.09	7.5		
GST	0.5	2.5	71.97	55.55	7.5		
GST	1.0	2.5	71.77	57.32	7.5		
GST	2.0	2.5	88.67	59.19	7.5		
GST	0.5	1.0	96.47	56.30	7.5		
GST	1.0	1.0	102.14	57.21	7.5		
GST	2.0	1.0	126.87	60.70	7.5		
GST	1.0	1.0	6.27	55.32	6.0		
GST	1.0	1.0	82.30	56.96	8.0		
GST	1.0	1.0	53.71	51.69	10.0		
GFP	0.5	5.0	88.24	81.58	7.5		
GFP	1.0	5.0	67.61	83.03	7.5		
GFP	2.0	5.0	90.62	84.32	7.5		
GFP	0.5	2.5	90.99	81.57	7.5		
GFP	1.0	2.5	69.89	83.05	7.5		
GFP	2.0	2.5	95.71	84.46	7.5		
GFP	0.5	1.0	95.15	82.14	7.5		
GFP	1.0	1.0	68.35	83.36	7.5		
GFP	2.0	1.0	93.75	84.49	7.5		
GFP	1.0	1.0	43.06	81.22	6.0		
GFP	1.0	1.0	78.48	82.99	8.0		
GFP	1.0	1.0	51.71	76.83	10.0		
			<b>GST</b>	<b>GFP</b>	<b>GST</b>	<b>GFP</b>	
GST-GFP	0.5	5.0	86.18	112.61	55.44	81.11	7.5
GST-GFP	1.0	5.0	91.55	125.87	56.51	82.49	7.5
GST-GFP	2.0	5.0	72.69	104.63	57.96	84.02	7.5
GST-GFP	0.5	2.5	46.96	61.08	54.44	81.23	7.5
GST-GFP	1.0	2.5	95.37	127.35	56.08	82.65	7.5

---

GST-GFP	2.0	2.5	67.80	91.54	57.52	84.02	7.5
GST-GFP	0.5	1.0	66.98	112.14	54.10	81.12	7.5
GST-GFP	1.0	1.0	72.43	78.94	55.49	83.19	7.5
GST-GFP	2.0	1.0	79.86	105.12	57.24	84.08	7.5
GST-GFP	1.0	1.0	60.22	67.45	55.17	79.86	6.0
GST-GFP	1.0	1.0	50.06	207.21	55.34	70.18	8.0
GST-GFP	1.0	1.0	70.29	131.12	52.81	76.15	10.0

---

802

803

804

805

806

807

808

809

810

811

812

813

814

815

816

817

818

819

Table 2 Dynamic weight loss (%) and degradation temperatures (°C) of samples (n=3, mean ± SD). The 1<sup>st</sup> represents water loss the remaining refer to weight loss due to other events, mainly degradation.

820

821

Samples	Dynamic weight loss (%)					Degradation temperatures (°C)			
	1 <sup>st</sup> (water loss)	2 <sup>nd</sup>	3 <sup>rd</sup>	4 <sup>th</sup>	Total	1st	2nd	3rd	4th
SA	18.2±0.7	36.3±0.5	10.3±0.9	-	64.9 ± 0.3	60.4±2.1	236.7±0.1	257.6±5.6	388.73±5.6
GLY	16.1±0.1	84.0±0.1	-	-	100.1± 0.1	79.7±1.4	220.4±2.0	-	-
BLK films	13.6±0.2	57.1±0.4	5.0±0.2	-	75.8±0.0	45.1±0.0	212.3±0.0	557.7±0.0	-
GFP films (30.2mg/g)	9.5±0.0	11.4±1.2	43.1±1.0	3.8±0.7	68.2±0.1	112.2±0.0	182.9±0.0	211.9±0.5	-
GFP films (6.6mg/g)	6.5±0.0	15.1±0.2	44.6±0.2	2.8±0.0	68.9±0.0	109.3±0.0	180.5±0.0	213.6±0.0	-
GFP films (3.3mg/g)	5.5±0.1	16.2±0.8	45.1±0.1	3.7±0.6	70.6±0.0	66.5±0.0	187.0±0.5	213.4±0.5	540.4±0.0
GST films (30.2mg/g)	16.7±0.1	49.9±0.0	-	-	66.6±0.2	59.8±0.01	209.4±0.1	-	-
GST films (6.6mg/g)	13.8±0.5	52.8±0.5	2.8±0.3	-	70.8±1.7	65.1±0.01	204.0±1.2	563.6±0.5	-
GST films (3.3mg/g)	14.7±0.5	50.8±0.0	3.1±0.6	2.3±0.9	70.9±0.8	53.9±2.3	197.7±1.2	370.9±0.5	-
GST-GFP films (3.3mg/g)	15.1±0.2	54.5±0.2	1.5±0.2	-	71.4±0.3	65.2±0.5	210.2±0.5	-	-
GST-GFP films (6.6mg/g)	11.9±0.2	16.7±0.6	42.4±0.5	3.4±0.3	74.5±0.3	62.2±0.5	182.6±2.6	208.6±0.5	568.6±1.6
GST-GFP films (3.3mg/g)	12.6±0.0	58.4±0.4	3.0±0.0	-	74.1±0.3	60.6±0.5	210.7±0.0	567.4±1.0	-

822 Table 3

823 (A) The effect of increasing plasticizer (GLY) on the mechanical (tensile) properties of blank  
824 SA films (mean  $\pm$  SD, n=3); (B) Mechanical (tensile) properties, % elongation at break,  
825 Young's modulus and tensile strength of optimized films (SA:GLY 1:2) loaded with proteins  
826 at different concentrations [mean  $\pm$  SD, (n = 3)].

827 (A)

<b>Films - Blank</b>	<b>% elongation at break (mean <math>\pm</math> SD)</b>	<b>Young's modulus (mPa) (mean <math>\pm</math> SD)</b>	<b>Tensile strength (N/mm<sup>2</sup>) (mean <math>\pm</math> SD)</b>
SA:GLY (1:0)	1.85 $\pm$ 0.19	20.77 $\pm$ 4.19	51.34 $\pm$ 6.76
SA:GLY (2:1)	5.37 $\pm$ 0.96	5.43 $\pm$ 2.00	21.26 $\pm$ 0.25
SA:GLY (4:3)	19.70 $\pm$ 1.77	3.21 $\pm$ 0.72	12.39 $\pm$ 0.43
SA:GLY (1:1)	7.43 $\pm$ 0.87	3.12 $\pm$ 2.62	9.04 $\pm$ 0.59
SA:GLY (2:3)	10.10 $\pm$ 2.12	0.80 $\pm$ 0.34	3.81 $\pm$ 0.51
SA:GLY (1:2)	38.84 $\pm$ 0.86	0.40 $\pm$ 0.08	6.12 $\pm$ 0.11

828 (B)

<b>Films – Drug loaded</b>	<b>% elongation at break (mean <math>\pm</math> SD)</b>	<b>Young's modulus (mPa) (mean <math>\pm</math> SD)</b>	<b>Tensile strength (N/mm<sup>2</sup>) (mean <math>\pm</math> SD)</b>
GST films (30.2mg/g)	11.76 $\pm$ 2.55	0.42 $\pm$ 0.14	4.07 $\pm$ 1.19
GST films (6.6mg/g)	5.46 $\pm$ 0.92	0.49 $\pm$ 0.13	2.56 $\pm$ 0.52
GST films (3.3mg/g)	6.20 $\pm$ 1.04	2.44 $\pm$ 0.35	6.36 $\pm$ 1.82
GST-GFP films (30.2mg/g)	20.74 $\pm$ 3.25	0.79 $\pm$ 0.18	5.04 $\pm$ 0.88
GST-GFP films (6.6mg/g)	23.38 $\pm$ 7.61	0.54 $\pm$ 0.07	4.77 $\pm$ 0.70
GST-GFP films (3.3mg/g)	19.04 $\pm$ 2.46	0.87 $\pm$ 0.21	4.50 $\pm$ 0.43
GFP films (30.2mg/g)	9.33 $\pm$ 0.66	0.88 $\pm$ 0.17	3.77 $\pm$ 0.87
GFP films (6.6mg/g)	7.78 $\pm$ 1.86	2.14 $\pm$ 0.34	6.16 $\pm$ 1.32
GFP films (3.3mg/g)	23.31 $\pm$ 4.04	0.97 $\pm$ 0.40	5.05 $\pm$ 0.33

829

Table 4 Release parameters obtained from fitting the dissolution data into different kinetic equations for the protein loaded film dressings

Protein loaded films	Zero order		First order		Higuchi		Korsmeyer-Peppas		
	$K_0$ (% min <sup>-1</sup> )	$R^2$	$K_1$ (min <sup>-1</sup> )	$R^2$	$K_H$ (% min <sup>-1/2</sup> )	$R^2$	$K_P$ (% min <sup>-n</sup> )	n	$R^2$
GST 6.6mg/g	0.242	0.906	-0.013	0.904	2.031	0.906	1.340	0.057	0.909
GFP 6.6mg/g	0.010	0.960	-0.001	0.977	0.223	0.986	1.330	0.016	0.986
GST- GFP 6.6mg/g	0.061	0.963	-0.002	0.961	0.615	0.922	1.021	0.020	0.922

$K_0$ ,  $K_1$ ,  $K_H$ ,  $K_P$  are the release rate constant for zero order, first order, Higuchi and Korsmeyer-Peppas kinetic models respectively, n is the release exponent and  $R^2$  is the correlation coefficient.

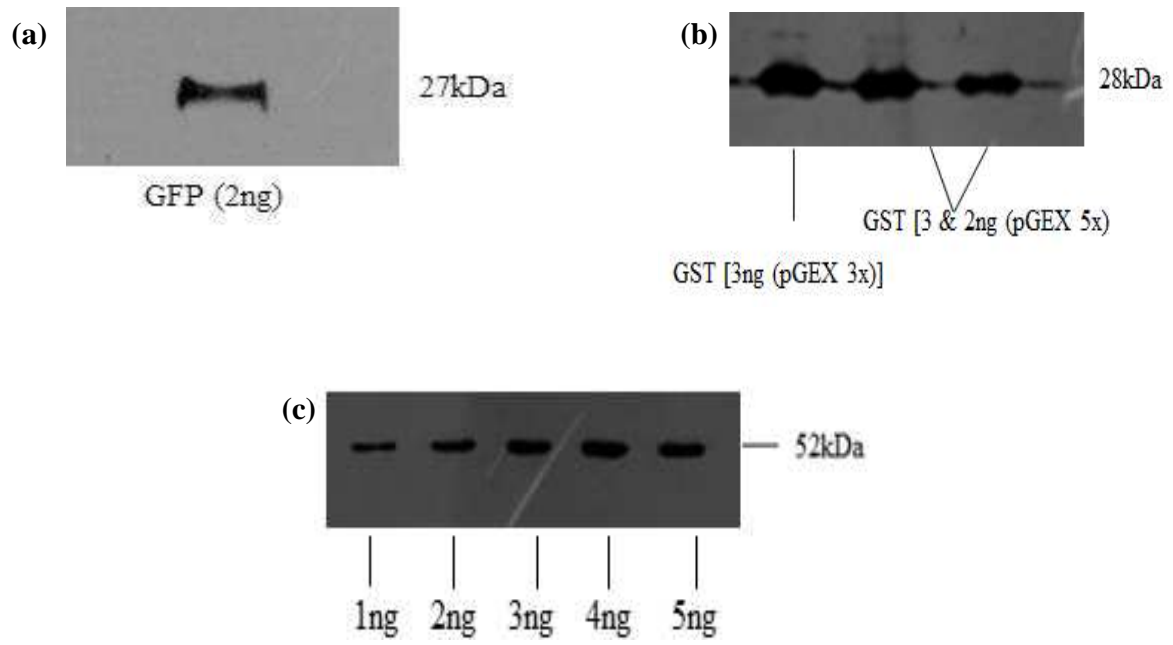


Fig. 1

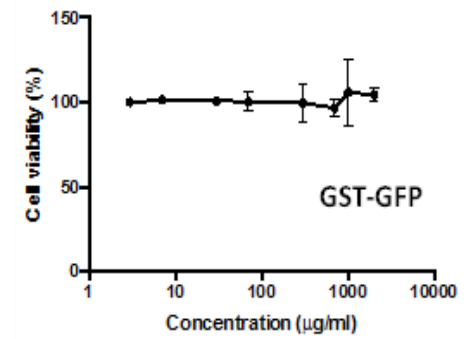
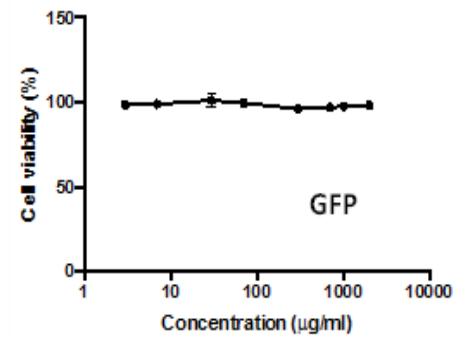
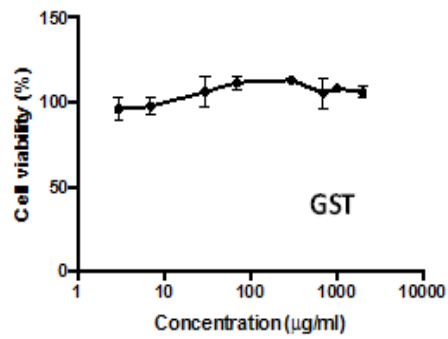
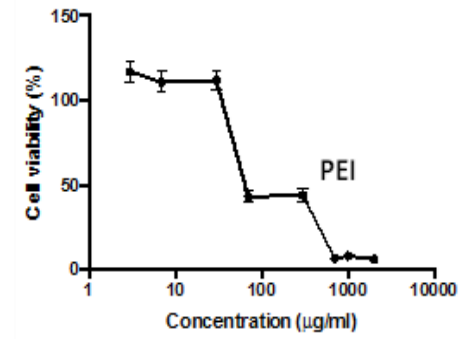
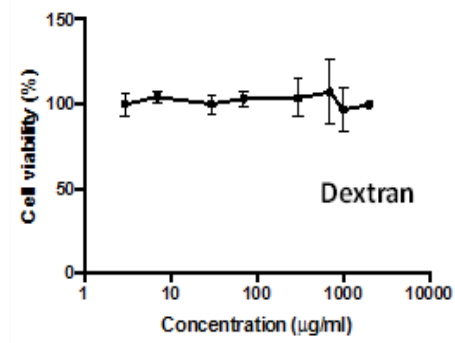
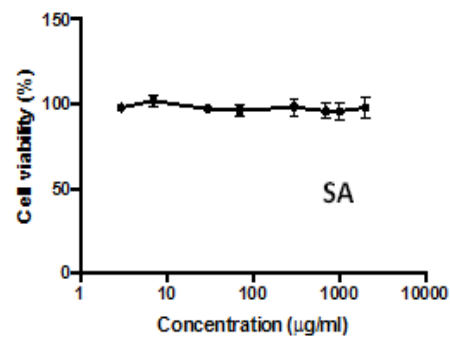
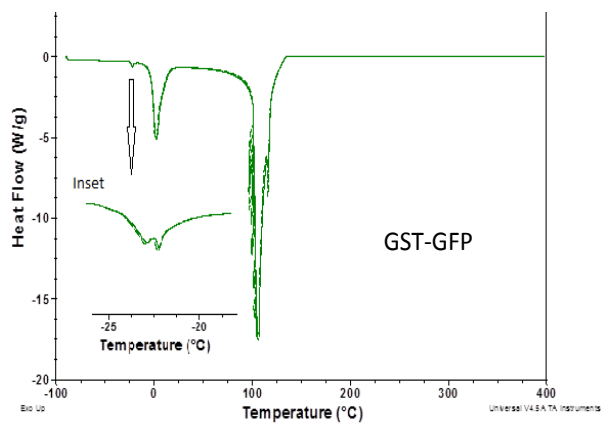
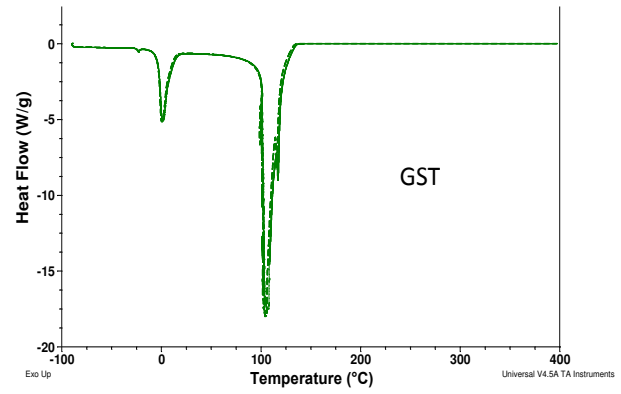
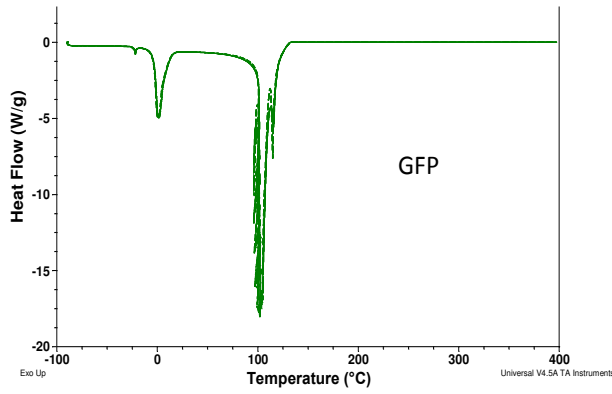
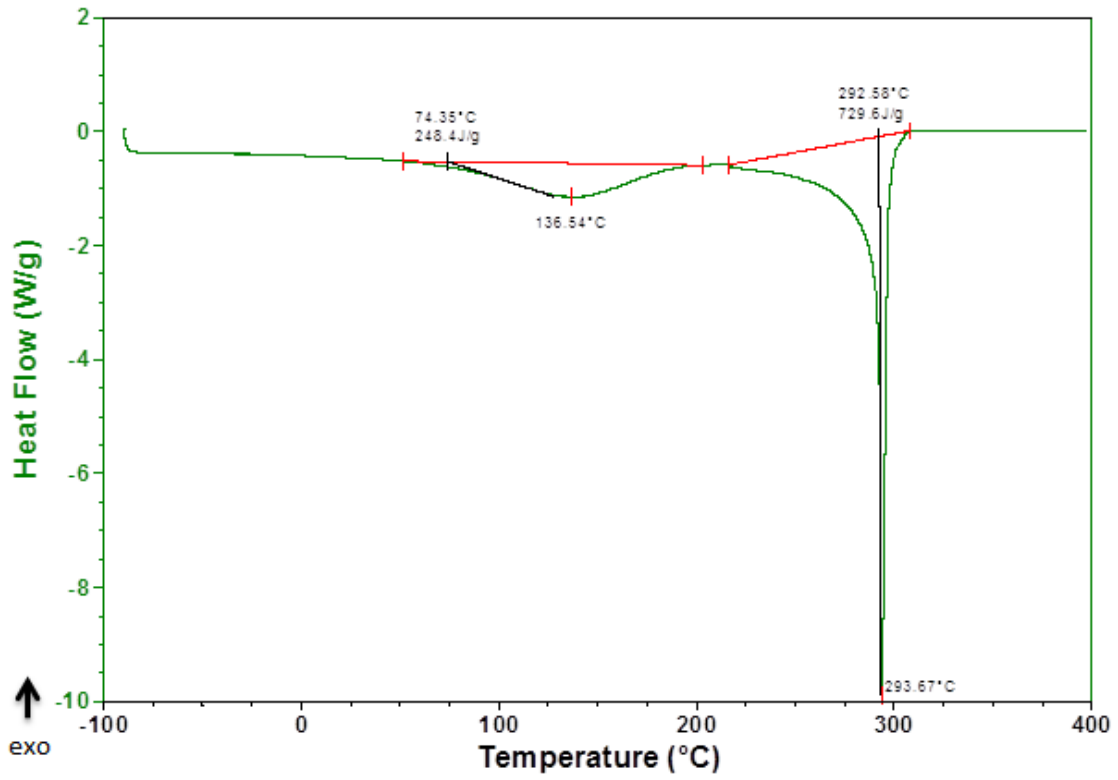


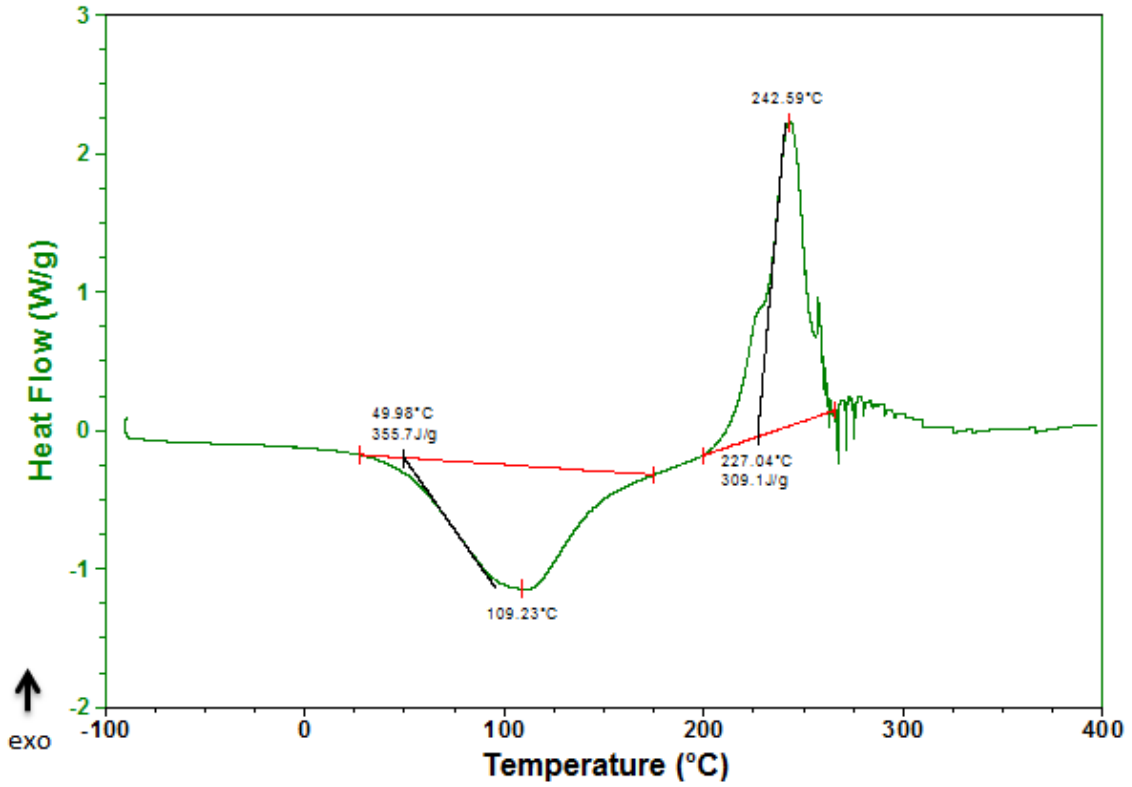
Fig. 2



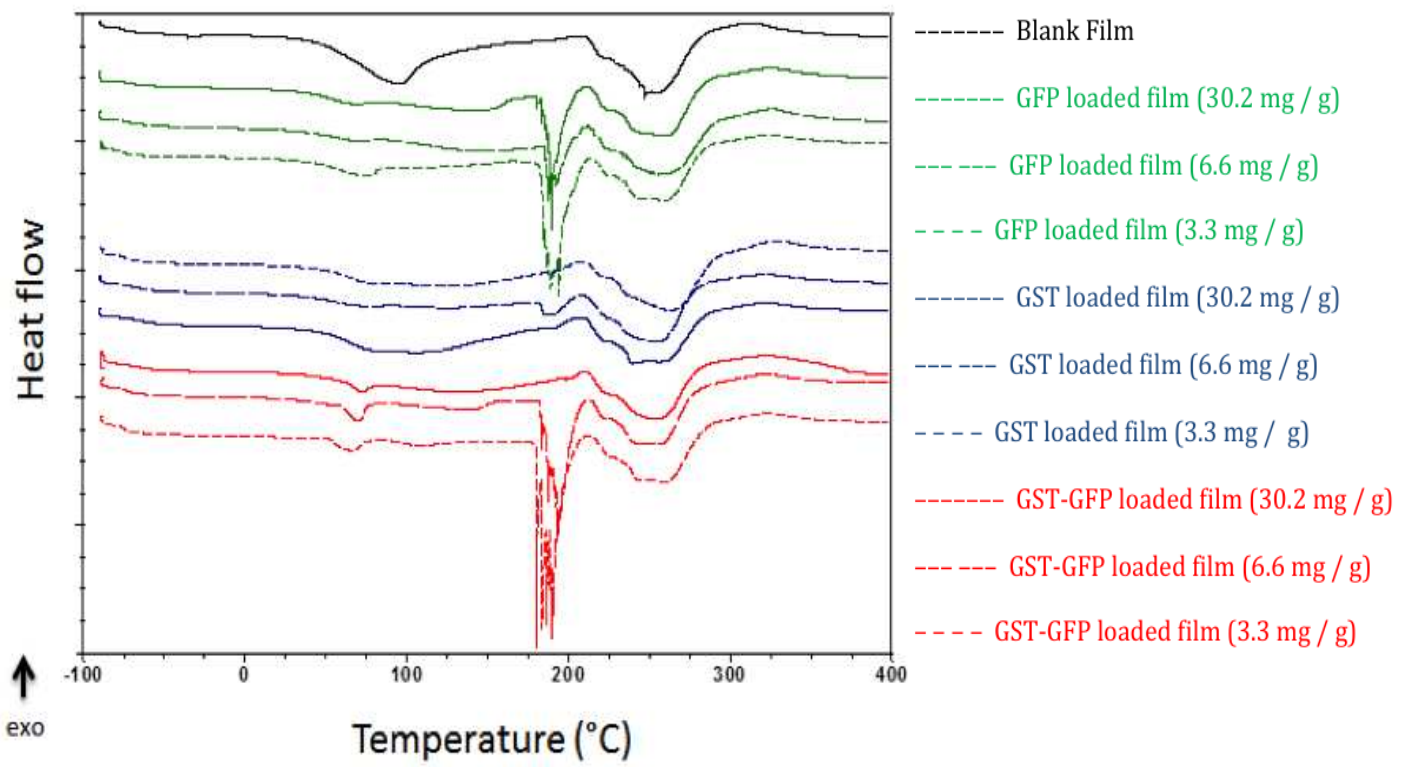
(A)



(B)



(C)



(D)

Fig. 3

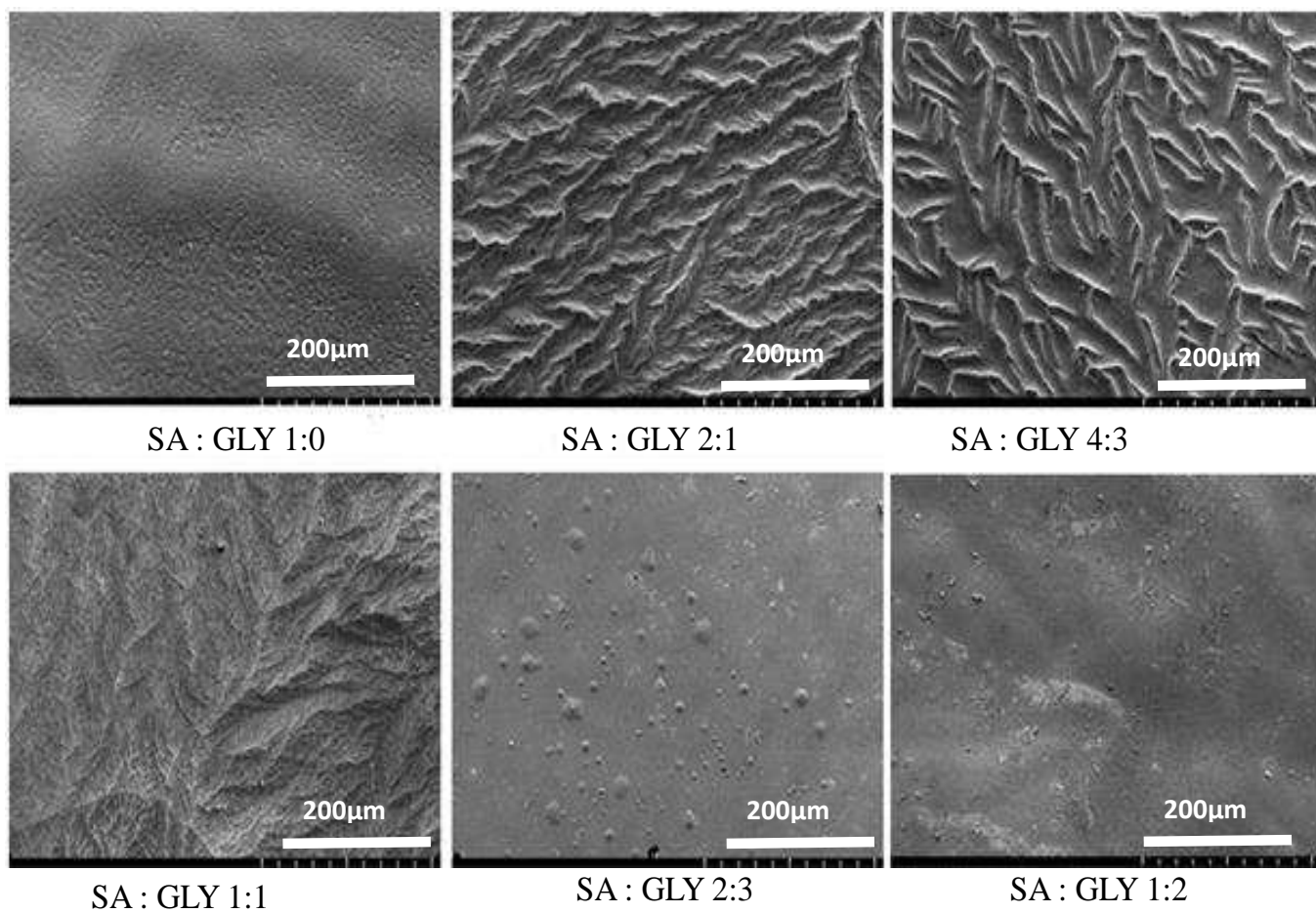


Fig. 4

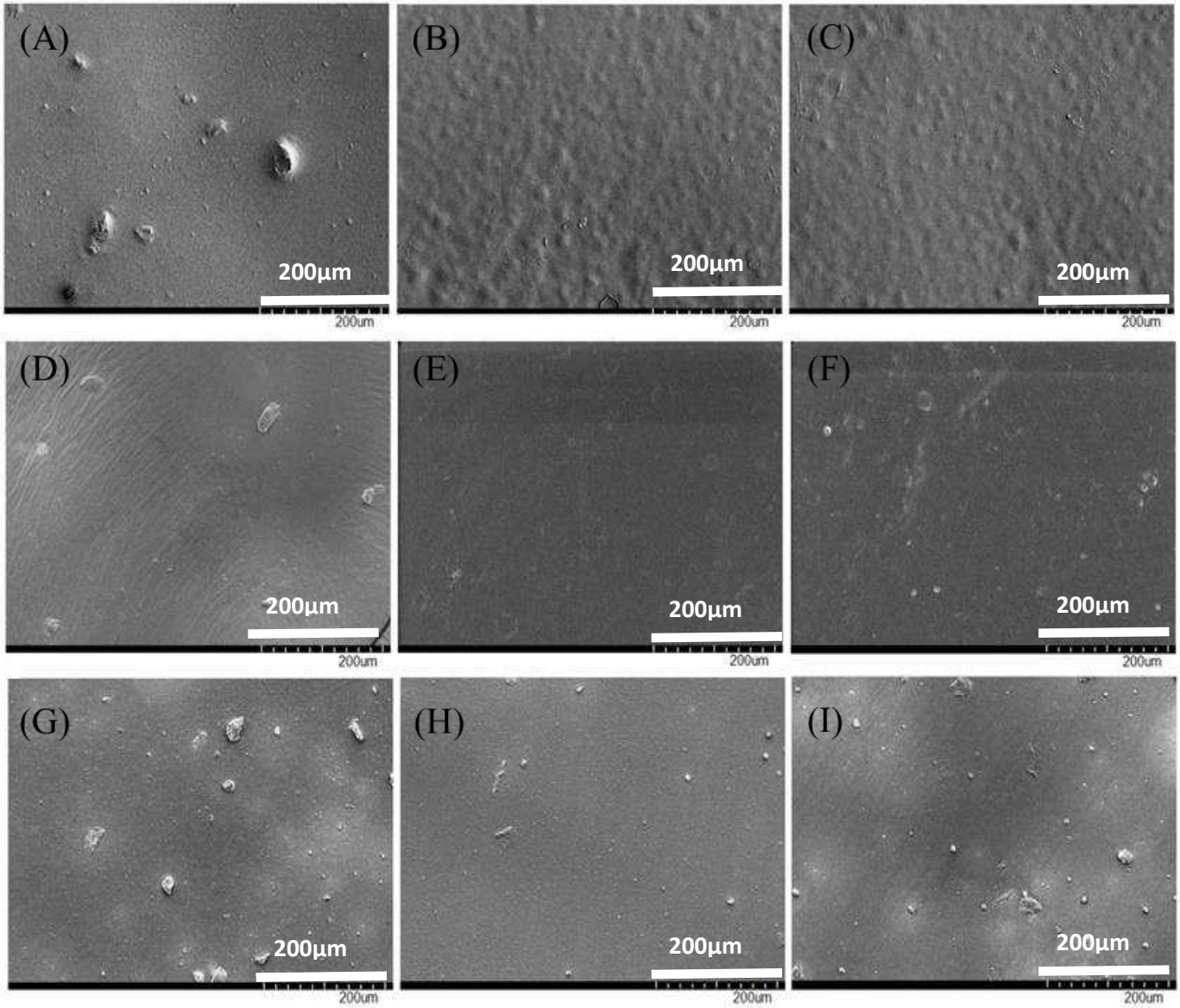


Fig. 5

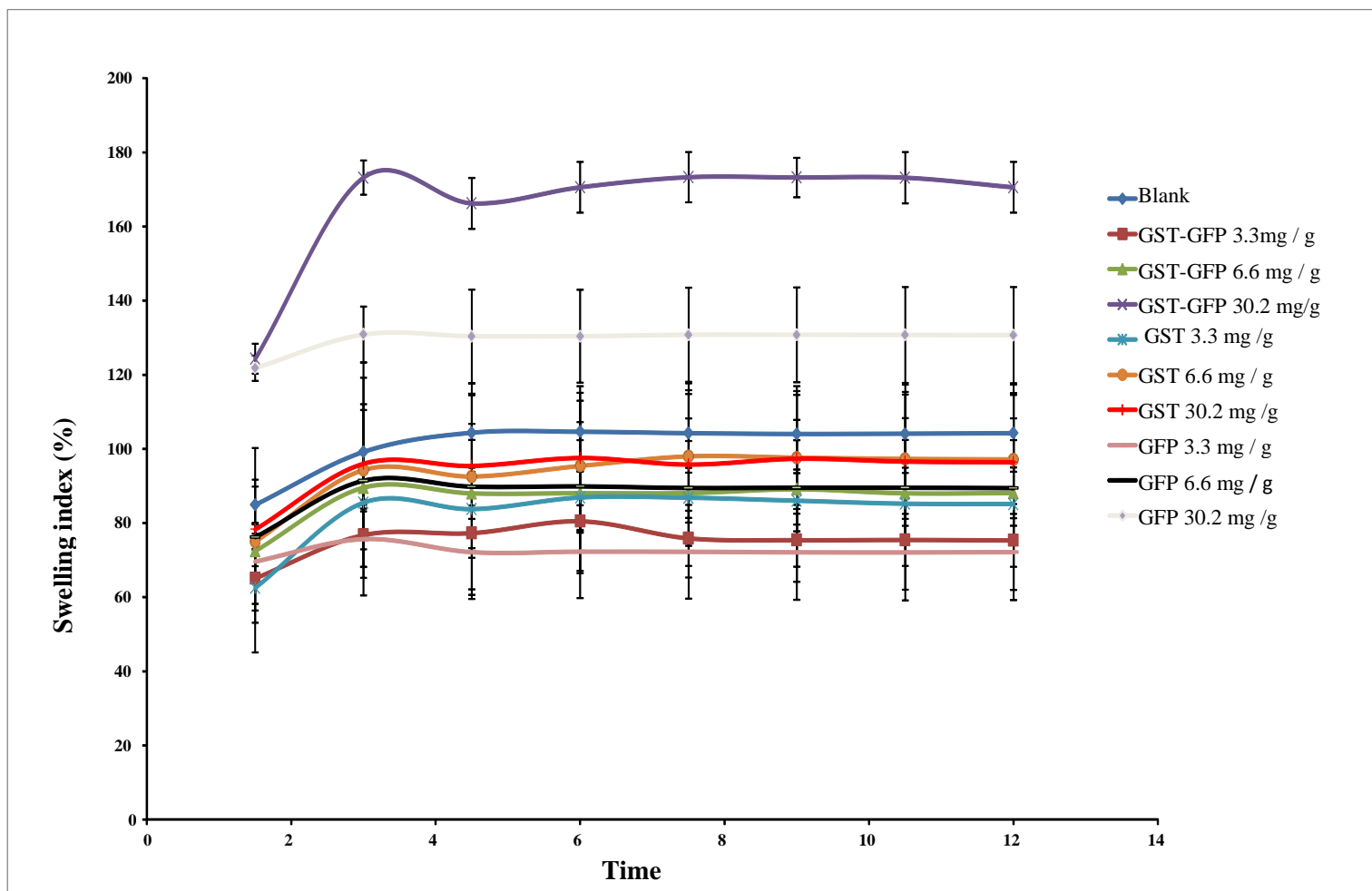


Fig. 6

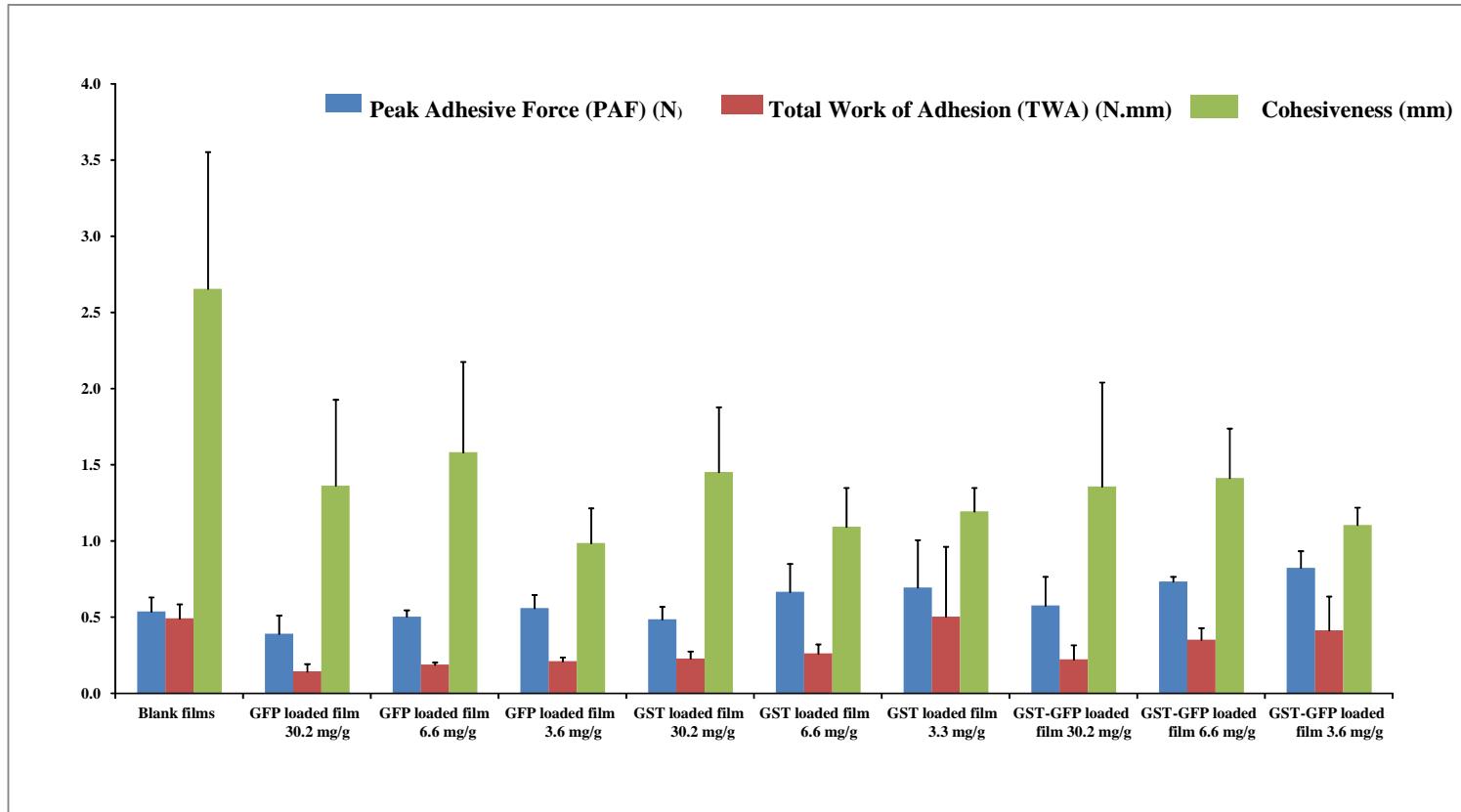


Fig. 7

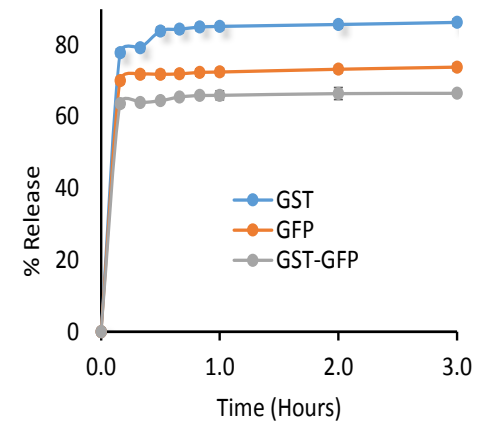
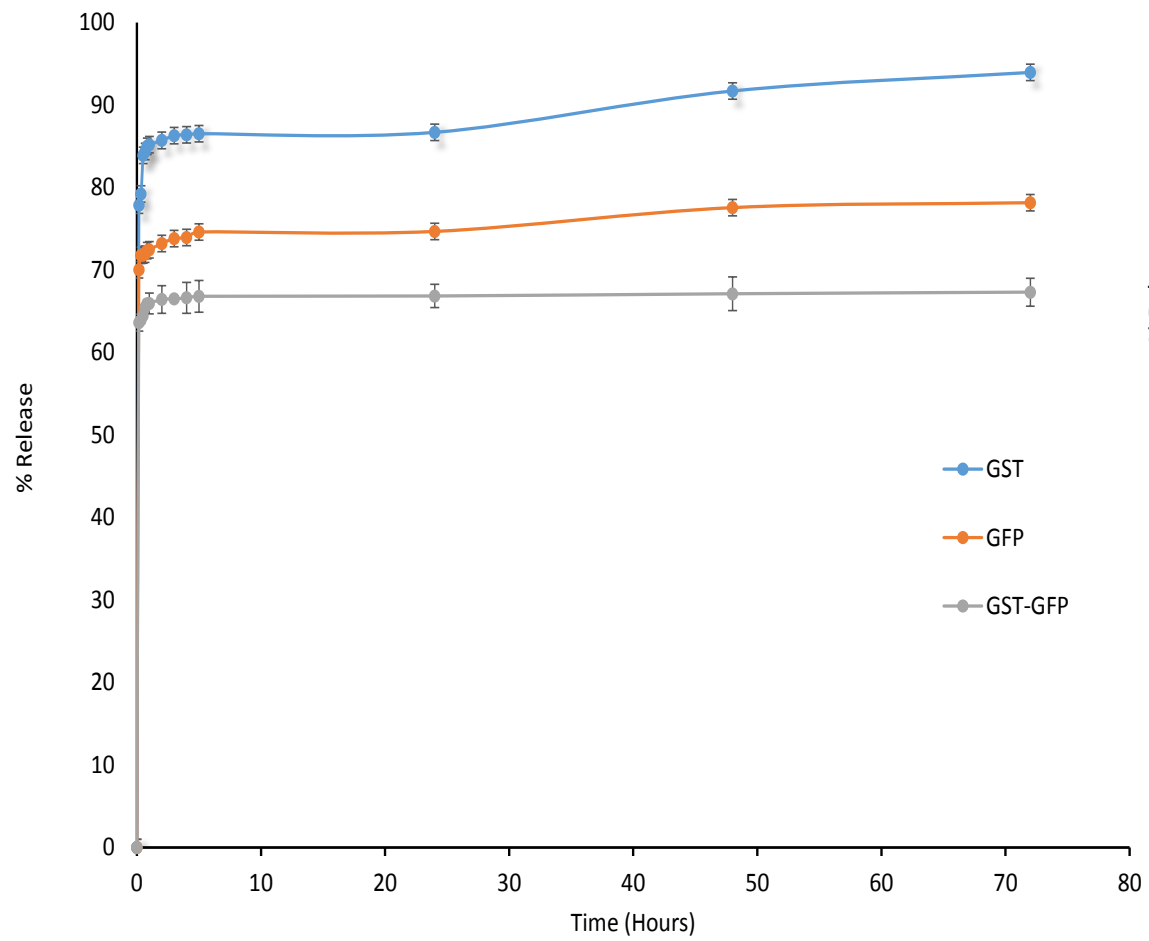


Fig. 8

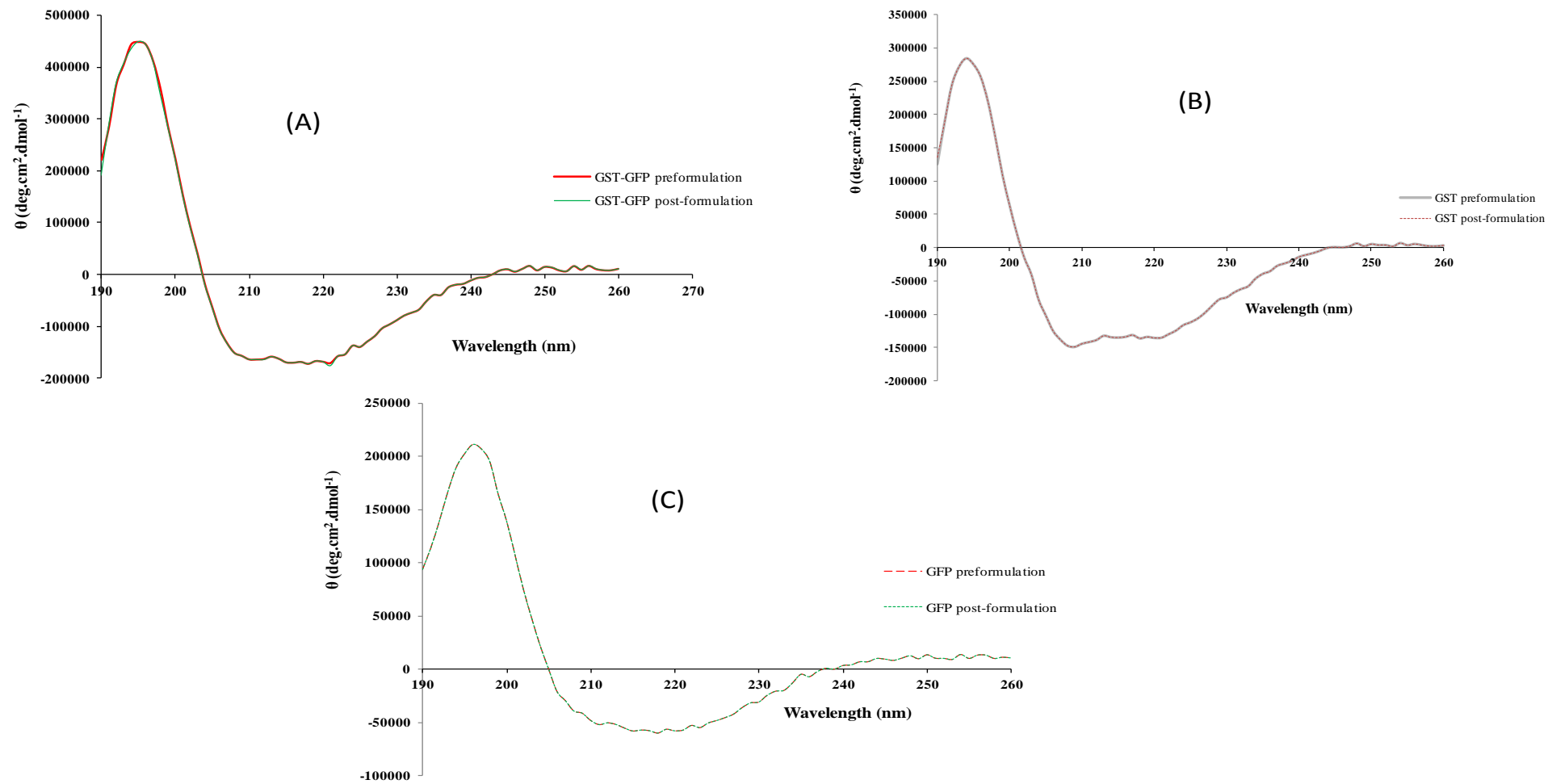


Fig. 9

## APPENDIX - SUPPLEMENTARY DATA

### A1 High sensitivity differential scanning calorimetry (HSDSC)

Generally, the results show that in all three proteins, an increase in scan rate from 0.5 to 2.0°C/minute increased the  $T_{\max}$  at pH 7.5 for the same protein concentration. From Table 1, it can also be seen that the optimum pH for the three proteins was 7.5 due to the higher  $T_{\max}$  observed when compared to that of the other pH values (6.0, 8.0 and 10.0). Further, Table 1 also shows that the optimum pH for the three proteins was 7.5 due to the higher  $T_{\max}$  observed when compared to that of the other pH values (6.0, 8.0 and 10.0). Comparing the  $T_{\max}$  of the individual proteins (GST, GFP) to the  $T_{\max}$  of the proteins within the construct (GST-GFP) at 1mg/mL and pH 7.5, it can be seen (Table 1) that GST was thermally more stable on its own than in the presence of GFP in the construct protein (GST-GFP) at all three scan rates (0.5, 1.0 and 2.0°C / minute). However, the  $T_{\max}$  for GFP alone and within the construct were similar at scan rates (1 and 2°C/minute) and differing by about 1.0°C at a scan rate 0.5°C/minute. Therefore, it can be concluded that GFP influenced the thermal stability of GST.

Enthalpy change ( $\Delta H$ ) fluctuated with scan rate for all three proteins which indicates that the rate of scanning influences the thermal denaturation process of the three proteins. Concentration also influenced  $\Delta H$  for all three proteins though there was no direct correlation. However, concentration did not influence the  $T_{\max}$  significantly and therefore a concentration of 1mg/mL was used for all three proteins to evaluate the effect of pH on the proteins thermal stability.

From Table 1, it can be seen that the optimum pH for the three proteins was 7.5 due to the higher  $T_{\max}$  observed when compared to that of the other pH values (6.0, 8.0 and 10.0). For example, in the case of GST, the  $T_{\max}$  at the different pHs (7.5, 6.0, 8.0 and 10.0), decreased

from 57.21°C (pH 7.5), 56.96°C (pH 8.0), 55.32°C (pH 6.0) to 51.69°C for pH 10.0. In addition,  $\Delta H$  decreased from 102.14, 82.30 kJ/mol, 53.71 kJ/mol and 6.27 kJ/mol for pH's (7.5, 8.0, 10.0 and 6.0) respectively, significantly reducing the enthalpy of the reaction. Similar results were also observed for GFP. However, for the construct protein (GST-GFP), the differences in  $T_{max}$  between pHs were not as high compared to the individual proteins (GST and GFP). The  $T_{max}$  ranged from 55.49°C, 55.34°C, 55.17°C for pH 7.5, 8.0, 6.0 respectively with about 3°C difference for pH 10.0 (52.81 kJ/mol). However, the difference in  $\Delta H$  was higher for all four pH values; 7.5 (72.43 kJ/mol), 10.0 (70.29 kJ/mol), 6.0 (60.22 kJ/mol) and 8.0 (50.06 kJ/mol). For GFP within the construct protein (GST-GFP),  $T_{max}$  values observed were 83.19°C, 79.86°C, 76.15°C and 70.18°C, at pH values of 7.5, 6.0, 10.0 and 8.0 respectively. Comparing the  $T_{max}$  of the individual proteins (GST, GFP) to the  $T_{max}$  of the proteins within the construct (GST-GFP) at 1mg/mL and pH 7.5, it can be seen (Table 1) that GST was thermally more stable on its own than in the presence of GFP in the construct protein (GST-GFP) at all three scan rates (0.5, 1.0 and 2.0°C / minute) with the difference in  $T_{max}$  between 2.0–3.0°C. However, the  $T_{max}$  for GFP alone and within the construct were similar at scan rates (1 and 2°C/minute) and differing by about 1.0°C at a scan rate 0.5°C/minute. Therefore, it can be concluded that GFP influenced the thermal stability of GST.

## A2 Differential scanning calorimetry (DSC)

The peaks around 100°C are associated with protein decomposition, however, at this temperature, all three protein would have denatured from their native state. This suggests that the peak at 100°C could be decomposition of denatured proteins but this may require further investigation. Peaks at around 0°C are due to thermal melting of the proteins as the temperature increased. The peak at approximately -20°C can be attributed to phase transition of the proteins in the crystal state prior to melt at 0°C. Both GST and GFP showed this phase transition at -

22.89°C and -22.09 respectively. However, GST-GFP produced two peaks at this phase that can be attributed to the presence of both GST and GFP in the recombinant GST-GFP.